

ON THE GENERALIZATION BEHAVIOR OF DEEP RESIDUAL NETWORKS FROM A DYNAMICAL SYSTEM PERSPECTIVE *

JINSHU HUANG[†], MINGFEI SUN[†], AND CHUNLIN WU^{†‡}

Abstract. Deep neural networks (DNNs) have significantly advanced machine learning, with model depth playing a central role in their successes. The dynamical system modeling approach has recently emerged as a powerful framework, offering new mathematical insights into the structure and learning behavior of DNNs. In this work, we establish generalization error bounds for both discrete- and continuous-time residual networks (ResNets) by combining Rademacher complexity, flow maps of dynamical systems, and the convergence behavior of ResNets in the deep-layer limit. The resulting bounds are of order $O(1/\sqrt{S})$ with respect to the number of training samples S , and include a structure-dependent negative term, yielding depth-uniform and asymptotic generalization bounds under milder assumptions. These findings provide a unified understanding of generalization across both discrete- and continuous-time ResNets, helping to close the gap in both the order of sample complexity and assumptions between the discrete- and continuous-time settings.

Key words. Deep learning, dynamical system, generalization bound, Rademacher complexity, asymptotic behavior

MSC codes. 68T07, 68Q87, 68V15, 37N99

1. Introduction. Deep learning has achieved remarkable successes across diverse applications in recent years. A key driver behind these successes is the increasing depth of neural networks, which enables the hierarchical extraction of complex features and representations [28, 16, 23]. Despite these empirical advances, the fundamental properties of deep neural networks (DNNs) remain not fully understood due to their inherent complexity. The expressivity and approximation, generalization, and optimization constitute the essential components of the mathematical mechanisms underlying deep learning [17]. Among them, understanding generalization behavior is one of the most important aspects, as it directly relates to the ability of DNNs to perform well on unseen data beyond the training set with a sample size S .

The generalization theory serves as a fundamental method for characterizing the predictive performance of DNNs on unseen data. Early works, such as [3, 15], proposed upper bounds on the Vapnik-Chervonenkis (VC) dimension for certain classes of DNNs, which are related to generalization theory. Later, Neyshabur et al.[37] derived a generalization bound of order $O(1/\sqrt{S})$ based on Rademacher complexity, with a coefficient exponentially depending on network depth in the case of ReLU networks. Bartlett et al.[1] introduced a spectral normalized margin-based bound for DNNs on the classification task, still of order $O(1/\sqrt{S})$ and with only polynomial dependence on network depth. A similar result was obtained by [36] in the probably approximately correct (PAC) Bayesian framework. Further studies have investigated the generalization behavior of ResNets [23]. Li et al.[31] derived tighter margin-based bounds for general architectures, including CNNs and ResNets, explicitly capturing the effects of depth, width, and Lipschitz continuity. He et al.[21] investigated the influence of residual connections on the hypothesis complexity via covering numbers, showing that, when the total number of layers is fixed, residual connections do not increase the hypothesis complexity compared to chain-like networks. These results all yield generalization bounds of order

*Submitted to the editors DATE.

Funding: XXX

[†]School of Mathematical Sciences, Nankai University, Tianjin, China. (huangjsh@mail.nankai.edu.cn, sunmf@mail.nankai.edu.cn, wucl@nankai.edu.cn).

[‡]Corresponding author.

$O(1/\sqrt{S})$, while the constants involved may still grow rapidly with architectural parameters like depth unless additional structural or norm-based constraints are imposed. From a different perspective, E, Ma, and Wang [12] studied the Rademacher complexity of residual networks under a weighted path norm constraint, and derived generalization bounds of order $O(1/\sqrt{S})$ without explicit dependence on the network depth. Their analysis highlights the role of norm-based capacity control in mitigating the adverse effects of depth and width, and provides insight into why deep and wide ResNets can still generalize well in practice. Some other research investigates the impact of training algorithms on generalization performance [7, 27, 45], often leveraging algorithmic stability or robustness to derive generalization bounds, which typically do not improve upon the standard rate of order $O(1/\sqrt{S})$.

From the viewpoint of neural ordinary differential equations (ODEs) [8], Marion [34] used a covering number reasoning approach to establish generalization bounds for a class of continuous-time models with time-varying weights under the assumption of Lipschitz continuity in time. The resulting bounds given in [34] are of sample dependence of order $O(1/\sqrt[4]{S})$. Closely related to Marion [34], Bleistein and Guilloux [6] studied the generalization properties of Neural Controlled Differential Equations (NCDEs), which model supervised learning from irregularly sampled time series via controlled differential equations. Using continuity properties of CDE flows and Lipschitz-based complexity arguments similar to those in [34], they derived generalization bounds of order $O(1/\sqrt[4]{S})$ under suitable assumptions. More recently, Hanson and Raginsky [20] analyzed the generalization properties of neural ODEs through a Chen–Fliess series expansion, which represents continuous-depth models as infinitely wide, single-layer networks whose features are given by iterated Lie derivatives. This reformulation enables a compact analysis of the Rademacher complexity of neural ODEs and leads to generalization bounds of order $O(1/\sqrt{S})$. While this approach provides sharp sample complexity guarantees for continuous-depth models, it does not address the relationship between discrete-time ResNets and their continuous-depth limits, nor does it study the consistency of generalization behavior with respect to network depth. We note that, despite these recent advances for continuous-depth models, existing analyses do not yet provide a unified and depth-consistent generalization theory that simultaneously covers discrete-time ResNets and their continuous-time limits with matching $O(1/\sqrt{S})$ sample dependence. **In this work, we aim to study the consistency of generalization behavior of ResNets in the deep-layer limit, and establish depth-uniform generalization error bounds that are compatible for both discrete-time ResNets and their continuous-time limit models.**

Recently, a dynamical system modeling approach for DNNs has been proposed, offering a new mathematical explanation of their structural and learning properties, and enabling asymptotic analysis as the number of layers tends to infinity. The pioneering works [11, 19] revealed that ResNets [23] can be interpreted as discrete-time approximations of ODEs. This interpretation has inspired subsequent research yielding both theoretical insights [5, 43, 32, 30] and practical innovations like architecture design [19, 33, 40] and training algorithms [8, 39, 18]. For instances, [30] investigates continuous-time ResNets and establishes general sufficient conditions for their universal approximation capabilities in L^p spaces from the approximation perspective, while Li et al. [32] studied the approximation and optimization theory of linear continuous-time recurrent neural networks (RNNs), providing a rigorous characterization of the relationship between memory structures and learning efficiency in linear dynamical models. Furthermore, the dynamical system perspective enables the analysis of the asymptotic behavior of deep networks by establishing the convergence of discrete-time learning problems to their continuous-time counterparts [46, 24, 25], thereby providing a theoretical foundation for understanding the stability and convergence of the

learning problems of DNNs in the deep-layer limit. In this context, the term “dynamical system framework” refers to a unified modeling and analytical viewpoint that encompasses both discrete-time ResNets and their continuous-time limits.

In this paper, we study the generalization behavior of ResNets within the dynamical system modeling framework [11, 19]. In contrast to approaches that start directly from continuous-time neural ODEs, our analysis proceeds from discrete ResNets and exploits their convergence to continuous-time dynamics. This enables us to examine the asymptotic behavior of generalization error with growing network depth, revealing a novel link between architectural stability and generalization in the deep-layer limit. Our contributions are summarized as follows:

- (i) Within a dynamical system modeling framework, we establish generalization error bounds simultaneously for both discrete-time ResNets and their continuous-time counterparts. The resulting bounds are of optimal order $O(1/\sqrt{S})$ in both settings and are compatible across the discrete-to-continuous transition. In particular, they improve upon existing results that treat discrete- and continuous-time models jointly, such as [34], by providing sharper sample-complexity dependence.
- (ii) Our bounds are derived via a new contraction-type inequality for a broad class of activation functions, capturing structural properties beyond standard Lipschitz continuity. This leads to a refined bound structure consisting of a depth-independent leading term together with a non-positive, depth-dependent structural correction term induced by the activation functions. As a consequence, the generalization error admits an explicit depth-uniform upper bound.

These results imply that increasing network depth does not lead to an accumulation of generalization error, which is consistent with empirical observations of ResNets in practical applications. In contrast to prior works on discrete-time ResNets [31, 21], our analysis further admits an asymptotic interpretation as the network depth tends to infinity, suggesting that the generalization capacity of deep ResNets can remain stable in the deep-layer limit. Moreover, compared to continuous-time analyses based on the neural ODE perspective [20], our approach is grounded in a dynamical system framework that treats discrete- and continuous-time ResNets in a unified manner. We also validate our theoretical results through experiments on CIFAR10 and CIFAR100 image classification tasks.

The remainder of this paper is organized as follows. Section 2 formulates the generalization problem for discrete- and continuous-time ResNets. In Section 3, we present our main theoretical results, including generalization bounds for discrete- and continuous-time ResNets. Section 4 provides detailed proofs. In Section 5, we present some simple numerical experiments to validate the results. Finally, Section 6 concludes the paper.

2. Notations and problem formulation. In this section, we give some notations and introduce the learning problems for ResNets from the dynamical system viewpoint. Then we describe the generalization problem in neural network supervised learning.

2.1. Notations. Throughout this paper, we adopt the following notations. Let \mathbb{N} and \mathbb{R} denote the set of natural and real numbers, respectively. Scalars are denoted with italic letters (e.g., $N \in \mathbb{N}$), vectors and matrices are denoted with lowercase and capital in straight letters (e.g., $\mathbf{c} \in \mathbb{R}^N$ and $\mathbf{W} \in \mathbb{R}^{N \times N}$). Vector- and matrix-valued functions of time variable t are written in boldface, like $\mathbf{c}(\cdot)$ and $\mathbf{W}(\cdot)$. For a Lipschitz continuous function f , its Lipschitz constant is denoted by Lip_f . The i -th element of vector \mathbf{c} is written as c_i , and the i -th row of matrix \mathbf{C} is $\mathbf{C}_{i,\cdot}$. The l^∞ and l^2 norms for vectors or matrices in Euclidean space are denoted as $\|\cdot\|_\infty$ and $\|\cdot\|_2$, respectively. Let \mathcal{X} be a vector space. The notation \mathcal{X}^N represents the Cartesian product space of

$\underbrace{\mathcal{X} \times \dots \times \mathcal{X}}_N$. The characteristic function of the set Λ is denoted as $\mathbf{1}_\Lambda(\cdot)$. The space of functions that are continuous on $\Omega \subset \mathbb{R}^d$ is denoted by $\mathcal{C}(\Omega)$. The Sobolev space of functions that are q -times weakly differentiable and each weak derivative is \mathcal{L}^2 integrable on Ω is denoted by $\mathcal{H}^q(\Omega)$. For the reader's convenience, the key notations used throughout the paper are summarized in Table 1.

TABLE 1
Summary of key notations and their first appearances in the paper.

Symbol	Meaning	Appears in
n_d/n	Dimension of input/output	Subsection 2.2
L	Number of layers	Eq. (2.1)
τ_L	Discretization step	Eq. (2.1)
Θ_L^{total}	Discrete-time learnable parameter	Subsection 2.2
$x^l(\cdot; \Theta_L^{\text{total}})$	Output function of the l -th layer in Eq.(2.1) with Θ_L^{total}	Subsection 2.2
\mathcal{F}^l	Hypothesis set of discrete-time ResNet at l -th	Eq. (2.3)
T	Terminal time	Eq. (2.5)
Θ^{total}	Continuous-time learnable parameter	Subsection 2.2
$\mathbf{x}(T; \cdot; \Theta^{\text{total}})$	Output function of Eq.(2.5) with Θ^{total}	Subsection 2.2
\mathcal{F}^T	Hypothesis set of continuous-time ResNet at time T	Eq. (2.7)
$\Omega_{\Theta_L^{\text{total}}}/\Omega_{\Theta^{\text{total}}}$	Discrete/Continuous time parameter set	Subsection 2.2
ℓ	Loss function	Eq. (2.9)
\mathcal{D}/\mathcal{S}	Data distribution/Training sample set	Subsection 2.3
$\mathfrak{R}_{\mathcal{D}}(\cdot)/\hat{\mathfrak{R}}_{\mathcal{S}}(\cdot)$	Expected/Empirical loss (risk)	Eq. (2.9)/(2.10)
S	Number of training samples	Subsection 2.3
$GE_{\mathcal{S}}(\cdot)$	Generalization gap	Eq. (2.11)
$\mathcal{A}(\mathbb{R})$	Set of activation functions	Definition 3.1
Lip_{ψ}	Lipschitz constant of function ψ	Proposition 3.1
$\mathcal{R}_{\mathcal{Z}}(\mathcal{F})$	Rademacher complexity of function class \mathcal{F}	Proposition 3.2
B_{in}	Bound on the data distribution	Assumption A1
B_{Θ}	Bound on the learnable parameters	Assumption A2
κ	Local Lipschitz bound function for $\ell(\cdot, \mathbf{g})$	Assumption A4
B_{κ}/B_{ℓ}	Bound of κ/ℓ on some compact set	Theorem 3.5

2.2. Residual neural network and its dynamical system modeling. We present the dynamical system modeling of ResNets [11, 19]. In particular, we consider

$$(2.1) \quad \begin{aligned} x^{l+1} &= x^l + \tau_L [W^l \psi \circ (V^l x^l + b^l) + c^l], \quad 0 \leq l \leq L-1, \\ x^0 &= \psi \circ (Ud + a), \end{aligned}$$

where $d \in \mathbb{R}^{n_d}$ is the input data; $\psi : \mathbb{R} \rightarrow \mathbb{R}$ is the activation function, and is applied elementwise to vectors; the parameters $(U, a) =: \Theta^{\text{pre}} \in \mathcal{E}^{\text{pre}} =: \mathbb{R}^{n \times n_d} \times \mathbb{R}^n$ are learnable parameters in the preprocessing layer, and the parameters $(V^l, W^l, b^l, c^l) =: \Theta^l \in \mathcal{E} := \mathbb{R}^{m \times n} \times \mathbb{R}^{n \times m} \times \mathbb{R}^m \times \mathbb{R}^n$ are learnable parameters in l -th layer of ResNet; $L \in \mathbb{N}$ is the total layer number; $\tau_L = T/L$ is the discretization step, which serves as a ‘‘scaling factor’’.

Denote $\Theta_L = (\Theta_L^0, \Theta_L^1, \dots, \Theta_L^{L-1}) \in \mathcal{E}^L$. Let $\Theta_L^{\text{total}} = (\Theta^{\text{pre}}, \Theta_L) \in \mathcal{E}^{\text{pre}} \times \mathcal{E}^L$ be the learnable parameters for the ResNet (2.1) with L layers. Let $\Omega_{\Theta_L^{\text{total}}} \subset \mathcal{E}^{\text{pre}} \times \mathcal{E}^L$ be the parameter set. We denote $\|\Theta_L^l\|_\infty = \max\{\|\mathbf{V}^l\|_\infty, \|\mathbf{W}^l\|_\infty, \|\mathbf{b}^l\|_\infty, \|\mathbf{c}^l\|_\infty\}$, and define a norm for $\Theta_L^{\text{total}} \in \mathcal{E}^{\text{pre}} \times \mathcal{E}^L$ as

$$(2.2) \quad \|\Theta_L^{\text{total}}\|_\infty := \max\{\|\mathbf{U}\|_\infty, \|\mathbf{a}\|_\infty, \max_{0 \leq l \leq L-1} \|\Theta_L^l\|_\infty\}.$$

We rewrite the state variable \mathbf{x}^l in Eq.(2.1) as $\mathbf{x}^l(\mathbf{d}; \Theta_L^{\text{total}})$ ($0 \leq l \leq L$) to emphasize its dependency on the input data \mathbf{d} and the learnable parameter Θ_L^{total} and denote $x_i^l(\mathbf{d}; \Theta_L^{\text{total}})$ as the i -th element of $\mathbf{x}^l(\mathbf{d}; \Theta_L^{\text{total}})$. Therefore $\mathbf{x}^l(\mathbf{d}; \Theta_L^{\text{total}})$ can be seen as the functions from \mathbb{R}^{n_d} to \mathbb{R}^n when the parameter Θ_L^{total} is given, and we can define the hypothesis set of discrete-time ResNet at l -th ($0 \leq l \leq L$) layer as

$$(2.3) \quad \mathcal{F}^l := \{\mathbf{x}^l(\cdot; \Theta_L^{\text{total}}) \mid \mathbf{x}^l(\cdot; \Theta_L^{\text{total}}) : \mathbb{R}^{n_d} \rightarrow \mathbb{R}^n \text{ is the output function of the } l\text{-th layer in Eq.(2.1) with parameter } \Theta_L^{\text{total}} \in \Omega_{\Theta_L^{\text{total}}}\}.$$

The class of scalar functions representing the i -th component ($1 \leq i \leq n$) of the state variable at layer l is defined as

$$(2.4) \quad \mathcal{F}_i^l := \{x_i^l(\cdot; \Theta_L^{\text{total}}) \mid x_i^l(\cdot; \Theta_L^{\text{total}}) : \mathbb{R}^{n_d} \rightarrow \mathbb{R} \text{ is the } i\text{-th component of } \mathbf{x}^l(\cdot; \Theta_L^{\text{total}}) \text{ determined by Eq.(2.1) with parameter } \Theta_L^{\text{total}} \in \Omega_{\Theta_L^{\text{total}}}\}.$$

Note that the hypothesis classes \mathcal{F}^l and \mathcal{F}_i^l ($0 \leq l \leq L$) consist of vector-valued and scalar-valued functions induced by deep neural networks with residual architectures as given in Eq.(2.1), and parameterized by parameters in $\Omega_{\Theta_L^{\text{total}}}$. For notational simplicity, we omit the explicit dependence of the hypothesis sets on the parameter set, as $\Omega_{\Theta_L^{\text{total}}}$ is fixed throughout the paper.

The dynamical system approach modeled the discrete-time ResNet Eq.(2.1) as a continuous-time ODE [11, 19]. Therefore, we consider the following continuous-time counterpart of Eq.(2.1)

$$(2.5) \quad \begin{aligned} \frac{d\mathbf{x}(t)}{dt} &= \mathbf{W}(t)\psi \circ (\mathbf{V}(t)\mathbf{x}(t) + \mathbf{b}(t)) + \mathbf{c}(t), t \in [0, T], \\ \mathbf{x}(0) &= \psi \circ (\mathbf{U}\mathbf{d} + \mathbf{a}). \end{aligned}$$

Similar to the discrete-time case, the learnable parameters of (2.5) are packaged as $\Theta^{\text{total}} = (\Theta^{\text{pre}}, \Theta)$, where $\Theta^{\text{pre}} = (\mathbf{U}, \mathbf{a})$, $\Theta(t) = (\mathbf{V}(t), \mathbf{W}(t), \mathbf{b}(t), \mathbf{c}(t)) \in \mathcal{E}, t \in [0, T]$. We then consider the parameter space of Θ as $\mathcal{C}([0, T]; \mathcal{E}) \cap \mathcal{H}^1(0, T; \mathcal{E})$ and denote

$$\begin{aligned} \|\Theta\|_{\mathcal{C}} &:= \max\{\max_{0 \leq t \leq T} \|\mathbf{V}(t)\|_\infty, \max_{0 \leq t \leq T} \|\mathbf{W}(t)\|_\infty, \max_{0 \leq t \leq T} \|\mathbf{b}(t)\|_\infty, \max_{0 \leq t \leq T} \|\mathbf{c}(t)\|_\infty\}; \\ \|\Theta\|_{\mathcal{H}^1} &:= \max\{\|\mathbf{V}\|_{\mathcal{H}^1}, \|\mathbf{W}\|_{\mathcal{H}^1}, \|\mathbf{b}\|_{\mathcal{H}^1}, \|\mathbf{c}\|_{\mathcal{H}^1}\}. \end{aligned}$$

Then, for $\Theta^{\text{total}} = (\Theta^{\text{pre}}, \Theta) \in \mathcal{E}^{\text{pre}} \times (\mathcal{C}([0, T]; \mathcal{E}) \cap \mathcal{H}^1(0, T; \mathcal{E}))$, a norm is given as

$$(2.6) \quad \|\Theta^{\text{total}}\| = \max\{\|\mathbf{U}\|_\infty, \|\mathbf{a}\|_\infty, \|\Theta\|_{\mathcal{C}}, \|\Theta\|_{\mathcal{H}^1}\}.$$

The set of learnable parameters is $\Omega_{\Theta^{\text{total}}} \subset \mathcal{E}^{\text{pre}} \times (\mathcal{C}([0, T]; \mathcal{E}) \cap \mathcal{H}^1(0, T; \mathcal{E}))$.

We rewrite the states $\mathbf{x}(t)$ in Eq.(2.5) as the flow map notation $\mathbf{x}(t; \mathbf{d}; \Theta^{\text{total}})$ to emphasize its dependency on the input data \mathbf{d} and the learnable parameter Θ^{total} . Then the hypothesis set (or space) of continuous-time ResNet (2.5) is given as

$$(2.7) \quad \mathcal{F}^T = \{\mathbf{x}(T; \cdot; \Theta^{\text{total}}) \mid \mathbf{x}(T; \cdot; \Theta^{\text{total}}) : \mathbb{R}^{n_d} \rightarrow \mathbb{R}^n \text{ is the output function of Eq.(2.5) with parameter } \Theta^{\text{total}} \in \Omega_{\Theta^{\text{total}}}\};$$

and the class of scalar functions that represent the i -th component ($1 \leq i \leq n$) of the continuous-time state variable is defined as

$$(2.8) \quad \mathcal{F}_i^T = \{x_i(T; \cdot; \Theta^{\text{total}}) \mid x_i(T; \cdot; \Theta^{\text{total}}) : \mathbb{R}^{n_d} \rightarrow \mathbb{R} \text{ is the } i\text{-th component of } \mathbf{x}(T; \cdot; \Theta^{\text{total}}) \text{ determined by Eq.(2.5) with parameter } \Theta^{\text{total}} \in \Omega_{\Theta^{\text{total}}}\}.$$

Similar to the discrete-time case, we omit the dependence of the hypothesis sets on the parameter set, as $\Omega_{\Theta^{\text{total}}}$ is fixed throughout the paper.

2.3. The problem of generalization for discrete- and continuous-time ResNets. Let \mathfrak{D} be an (often unknown) probability distribution supported on a σ -algebra of $\mathbb{R}^{n_d} \times \mathbb{R}^n$. In supervised learning, the objective is to approximate a target function $f : \mathbb{R}^{n_d} \rightarrow \mathbb{R}^n$ that effectively ‘‘characterizes’’ \mathfrak{D} .

The target function is determined by solving the following optimal control problem

$$(2.9) \quad \inf_{\Theta_L^{\text{total}} \in \Omega_{\Theta_L^{\text{total}}}} \left\{ \mathfrak{R}_{\mathfrak{D}}(x^L(\cdot; \Theta_L^{\text{total}})) := \mathbb{E}_{(\mathbf{d}, \mathbf{g}) \sim \mathfrak{D}} [\ell(x^L(\mathbf{d}; \Theta_L^{\text{total}}), \mathbf{g})] \right\}$$

subject to : $x^L(\mathbf{d}; \Theta_L^{\text{total}})$ is the end state of Eq.(2.1) with input \mathbf{d} ,

where $\ell : \mathbb{R}^n \times \mathbb{R}^n \rightarrow [0, \infty)$ is a loss function, and $\mathfrak{R}_{\mathfrak{D}}(x^L(\cdot; \Theta_L^{\text{total}}))$ is the so-called expected loss or risk. Since the distribution \mathfrak{D} is unknown, this quantity cannot be computed directly. Instead, we approximate it using a training dataset $\mathcal{S} := \{(\mathbf{d}_{(s)}, \mathbf{g}_{(s)})\}_{s=1}^S$ consisting of independently and identically distributed (i.i.d.) samples drawn from \mathfrak{D} . The goal is then to find a hypothesis $x^L(\cdot; \Theta_L^{\text{total}})$ by solving the following sampled optimal control problem

$$(2.10) \quad \inf_{\Theta_L^{\text{total}} \in \Omega_{\Theta_L^{\text{total}}}} \left\{ \hat{\mathfrak{R}}_{\mathcal{S}}(x^L(\cdot; \Theta_L^{\text{total}})) := \frac{1}{S} \sum_{s=1}^S \ell(x^L(\mathbf{d}_{(s)}; \Theta_L^{\text{total}}), \mathbf{g}_{(s)}) \right\}$$

subject to : $x^L(\mathbf{d}_{(s)}; \Theta_L^{\text{total}})$ is the end state of Eq.(2.1) with input $\mathbf{d}_{(s)}$,

where $\hat{\mathfrak{R}}_{\mathcal{S}}(x^L(\cdot; \Theta_L^{\text{total}}))$ is the empirical risk of the hypothesis.

A fundamental question in generalization theory is to understand how minimizing the empirical risk $\hat{\mathfrak{R}}_{\mathcal{S}}(x^L(\cdot; \Theta_L^{\text{total}}))$ provides a meaningful approximation to minimizing the true risk $\mathfrak{R}_{\mathfrak{D}}(x^L(\cdot; \Theta_L^{\text{total}}))$. This can be characterized by the so-called generalization gap

$$(2.11) \quad GE_{\mathcal{S}}(x^L(\cdot; \Theta_L^{\text{total}})) := \mathfrak{R}_{\mathfrak{D}}(x^L(\cdot; \Theta_L^{\text{total}})) - \hat{\mathfrak{R}}_{\mathcal{S}}(x^L(\cdot; \Theta_L^{\text{total}})), \quad x^L(\cdot; \Theta_L^{\text{total}}) \in \mathcal{F}^L.$$

The generalization gap of continuous-time ResNet is similarly defined, i.e.,

$$(2.12) \quad GE_{\mathcal{S}}(\mathbf{x}(T; \cdot; \Theta^{\text{total}})) = \mathfrak{R}_{\mathfrak{D}}(\mathbf{x}(T; \cdot; \Theta^{\text{total}})) - \hat{\mathfrak{R}}_{\mathcal{S}}(\mathbf{x}(T; \cdot; \Theta^{\text{total}})), \quad \mathbf{x}(T; \cdot; \Theta^{\text{total}}) \in \mathcal{F}^T.$$

In this work, we aim to investigate the asymptotic generalization behavior of ResNets in the deep-layer limit by establishing compatible generalization error bounds simultaneously for discrete-time ResNets and their continuous-time counterparts.

3. Main results and application. Motivated by the dynamical system modeling approach, which offers valuable insights into the approximation behavior, structural stability, and depth variation behavior of DNNs, we establish generalization error bounds for discrete- and continuous-time ResNets. This captures their generalization behavior in the deep-layer limit. We begin by introducing a class of commonly used activation functions and develop a new contraction-type inequality that reflects their structural properties. This inequality plays a key role in controlling the Rademacher complexity of the hypothesis class, leading to sharper generalization error bounds.

DEFINITION 3.1. *Let $\Gamma(\mathbb{R})$ be a set of functions such that for any $\phi \in \Gamma(\mathbb{R})$, $\phi : \mathbb{R} \rightarrow \mathbb{R}$ is increasing, Lip_ϕ -Lipschitz, and $\phi(x) = 0$ for all $x \leq 0$. Then the set of activation functions $\mathcal{A}(\mathbb{R})$ is given as $\mathcal{A}(\mathbb{R}) = \{\psi(\cdot) = \phi_1(\cdot - \alpha) - \phi_2(-\cdot - \beta) \mid \phi_1, \phi_2 \in \Gamma(\mathbb{R}), \alpha, \beta \geq 0\}$.*

TABLE 2
Examples of activation functions in $\mathcal{A}(\mathbb{R})$. The parameters $a_1 \in [0, 1]$, $a_2, \lambda, \lambda_1, \lambda_2 > 0$.

Activation functions	ψ	ϕ_1	ϕ_2	(α, β)
ReLU [14]	$\begin{cases} x, & x \geq 0 \\ 0, & x < 0 \end{cases}$	$x\mathbf{1}_{[0, \infty)}(x)$	0	$(0, \beta)$
PReLU [22]	$\begin{cases} x, & x \geq 0 \\ a_1x, & x < 0 \end{cases}$	$x\mathbf{1}_{[0, \infty)}(x)$	$a_1x\mathbf{1}_{[0, \infty)}(x)$	$(0, 0)$
TReLU	$\begin{cases} x - \lambda, & x \geq \lambda \\ 0, & x < \lambda \end{cases}$	$x\mathbf{1}_{[0, \infty)}(x)$	0	(λ, β)
ELU [10]	$\begin{cases} x, & x \geq 0 \\ a_2(e^x - 1), & x < 0 \end{cases}$	$x\mathbf{1}_{[0, \infty)}(x)$	$-a_2(e^{-x} - 1) \cdot \mathbf{1}_{[0, \infty)}(x)$	$(0, 0)$
TEReLU [38]	$\begin{cases} x - \lambda_1, & x \geq \lambda_1 \\ 0, & -\lambda_2 < x < \lambda_1 \\ a_2(e^{x+\lambda_2} - 1), & x \leq -\lambda_2 \end{cases}$	$x\mathbf{1}_{[0, \infty)}(x)$	$-a_2(e^{-x} - 1) \cdot \mathbf{1}_{[0, \infty)}(x)$	(λ_1, λ_2)
\mathcal{T}_λ [4]	$\begin{cases} x - \lambda, & x \geq \lambda \\ 0, & -\lambda < x < \lambda \\ x + \lambda, & x \leq -\lambda \end{cases}$	$x\mathbf{1}_{[0, \infty)}(x)$	$x\mathbf{1}_{[0, \infty)}(x)$	(λ, λ)
$\mathcal{S}_{\lambda_1, \lambda_2}$	$\begin{cases} x - \lambda_1, & x \geq \lambda_1 \\ 0, & -\lambda_2 < x < \lambda_1 \\ x + \lambda_2, & x \leq -\lambda_2 \end{cases}$	$x\mathbf{1}_{[0, \infty)}(x)$	$x\mathbf{1}_{[0, \infty)}(x)$	(λ_1, λ_2)
Tanh [16]	$\frac{e^x - e^{-x}}{e^x + e^{-x}}$	$\frac{e^x - e^{-x}}{e^x + e^{-x}} \mathbf{1}_{[0, \infty)}(x)$	$\frac{e^x - e^{-x}}{e^x + e^{-x}} \mathbf{1}_{[0, \infty)}(x)$	$(0, 0)$

The set $\mathcal{A}(\mathbb{R})$ includes many commonly used activation functions, as summarized in Table 2. Any function $\psi \in \mathcal{A}(\mathbb{R})$ that can be written in the form $\psi = \phi_1(\cdot - \alpha) - \phi_2(-\cdot - \beta)$ with $\phi_1, \phi_2 \in \Gamma(\mathbb{R})$, is Lip_ψ -Lipschitz continuous, where $\text{Lip}_\psi = \max\{\text{Lip}_{\phi_1}, \text{Lip}_{\phi_2}\}$. Recall the definition of empirical Rademacher complexity in Appendix A.1, we derive a refined contraction inequality by using the decomposition structure of activation functions.

PROPOSITION 3.2. *Let \mathcal{G} be a set of functions mapping \mathbb{R}^N to \mathbb{R} . Consider a sample set $\mathcal{Z} = \{z_{(1)}, z_{(2)}, \dots, z_{(S)}\}$ from some distribution \mathfrak{B} and an activation function $\psi \in \mathcal{A}(\mathbb{R})$ of the form $\psi(\cdot) := \phi_1(\cdot - \alpha) - \phi_2(-\cdot - \beta)$, where $\phi_1, \phi_2 \in \Gamma(\mathbb{R})$ and $\alpha, \beta \geq 0$. Then there exists a constant $C_{\mathcal{Z}}$*

dependent on \mathcal{Z} , $0 \leq C_{\mathcal{Z}} \leq \min\{S, \frac{\text{Lip}_{\psi} S}{\text{Lip}_{\phi_1} \alpha + \text{Lip}_{\phi_2} \beta} \mathcal{R}_{\mathcal{Z}}(\mathcal{G})\}$ and

$$(3.1) \quad \mathcal{R}_{\mathcal{Z}}(\psi \circ \mathcal{G}) \leq \text{Lip}_{\psi} \cdot \mathcal{R}_{\mathcal{Z}}(\mathcal{G}) - \frac{\text{Lip}_{\phi_1} \alpha + \text{Lip}_{\phi_2} \beta}{S} C_{\mathcal{Z}},$$

where $\text{Lip}_{\psi} = \max\{\text{Lip}_{\phi_1}, \text{Lip}_{\phi_2}\}$, Lip_{ϕ_i} are Lipschitz constants of function ϕ_i .

Proof. The proof is given in Section 4.1. \square

Remark 3.3. Proposition 3.2 provides a refined characterization of the Rademacher complexity of composed function classes compared to the classical contraction inequality in [42, Lemma 26.9], which states that

$$(3.2) \quad \mathcal{R}_{\mathcal{Z}}(\psi \circ \mathcal{G}) \leq \text{Lip}_{\psi} \cdot \mathcal{R}_{\mathcal{Z}}(\mathcal{G}).$$

Moreover, the result in [44, Lemma 1] is a special case of the above proposition with $\psi = \mathcal{T}_{\lambda}$.

The following example shows that Proposition 3.2 does give a tighter bound than (3.2).

Example 3.1. Given constants $\alpha, \beta, \gamma, \eta > 0$ such that $0 < \max\{\alpha, \beta\} < \gamma$ and any sample set $\mathcal{Z} = \{z_{(s)} \mid z_{(s)} \in \mathbb{R}^N, \|z_{(s)}\|_2 = 1, s = 1, \dots, S\}$. Consider the function class

$$\mathcal{G} := \{c_1 \|\cdot\|_2 + c_2 : \mathbb{R}^N \rightarrow \mathbb{R} \mid (c_1, c_2) \in [0, \eta] \times [\alpha, \gamma] \text{ or } (c_1, c_2) \in [-\eta, 0] \times [-\gamma, -\beta]\},$$

and function $\psi(\cdot) = (\cdot - \alpha)\mathbf{1}_{[0, \infty)}(\cdot - \alpha) - (-\cdot - \beta)\mathbf{1}_{[0, \infty)}(-\cdot - \beta)$. Then

$$(3.3) \quad \begin{aligned} \mathcal{R}_{\mathcal{Z}}(\mathcal{G}) &= \frac{1}{2^{S-1}} (\eta + \gamma) \binom{S-1}{\lfloor \frac{S}{2} \rfloor}, \\ \mathcal{R}_{\mathcal{Z}}(\psi \circ \mathcal{G}) &= \frac{1}{2^S} (2\eta + 2\gamma - \beta - \alpha) \binom{S-1}{\lfloor \frac{S}{2} \rfloor}, \end{aligned}$$

and therefore $\mathcal{R}_{\mathcal{Z}}(\psi \circ \mathcal{G}) \leq \text{Lip}_{\psi} \mathcal{R}_{\mathcal{Z}}(\mathcal{G}) - \frac{\alpha + \beta}{S} \cdot \frac{S}{2^S} \binom{S-1}{\lfloor \frac{S}{2} \rfloor}$.

Proof. The proof is basic and is supplied in supplementary materials. \square

Next, we use contraction inequality (3.1) to derive a generalization error bound for the discrete-time ResNet and discuss its implications for the continuous-time ResNet. The following assumptions are required for the subsequent analysis.

- (A₁) (Bounded data distribution) The data distribution \mathfrak{D} is supported in a bounded set, i.e., for all $(d, g) \sim \mathfrak{D}$, $\|d\|_2 + \|g\|_2 \leq B_{\text{in}}$ for some $B_{\text{in}} > 0$.
- (A₂) (Bounded parameter set) For some $B_{\Theta} > 0$, the parameter sets are given by

$$\begin{aligned} \Omega_{\Theta_L^{\text{total}}} &= \{\Theta_L^{\text{total}} : \Theta_L^{\text{total}} \in \mathcal{E}^{\text{pre}} \times \mathcal{E}^L, \|\Theta_L^{\text{total}}\|_{\infty} \leq B_{\Theta}\}, \\ \Omega_{\Theta^{\text{total}}} &= \{\Theta^{\text{total}} : \Theta^{\text{total}} \in \mathcal{E}^{\text{pre}} \times (\mathcal{C}([0, T]; \mathcal{E}) \cap \mathcal{H}^1(0, T; \mathcal{E})), \|\Theta^{\text{total}}\| \leq B_{\Theta}\}. \end{aligned}$$

- (A₃) (Activation function) The activation function $\psi \in \mathcal{A}(\mathbb{R})$.
- (A₄) (Loss function) The loss function $\ell : \mathbb{R}^n \times \mathbb{R}^n \rightarrow [0, \infty)$ is continuous and satisfies a local Lipschitz condition for the first argument in the following sense. There exist a continuous function $\kappa : \mathbb{R}^n \times \mathbb{R}^n \times \mathbb{R}^n \rightarrow [0, \infty)$ such that for all $x, \tilde{x}, g \in \mathbb{R}^n$,

$$|\ell(x, g) - \ell(\tilde{x}, g)| \leq \kappa(x, \tilde{x}, g) \|x - \tilde{x}\|_2.$$

Remark 3.4. These assumptions are mild and commonly used in deep learning theory. In particular, the boundedness assumptions (A_1) and (A_2) are standard [9, 26, 41, 24]. A broad class of loss functions satisfies (A_4) . For example:

- In image inverse problems, the loss function is usually $\ell(x, g) = \|x - g\|_2^2$. Then we can take $\kappa(x, \tilde{x}, g) = \|x - g\|_2 + \|\tilde{x} - g\|_2$.
- In image classification tasks, the loss function is usually the ramp loss [42], which is Lip_ℓ -Lipschitz. Then we can take $\kappa(x, \tilde{x}, g) \equiv \text{Lip}_\ell$.

We now present our two main results. One is the generalization error for discrete-time ResNets, and the other is that for continuous-time ResNets.

THEOREM 3.5. (*Generalization error for discrete-time ResNets*) *Assume assumptions (A_1) - (A_4) hold. Let the activation function $\psi \in \mathcal{A}(\mathbb{R})$ with $\phi_1, \phi_2 \in \Gamma(\mathbb{R})$ and $\alpha, \beta > 0$. Then there are constants C_S^l dependent on data \mathcal{S} , $0 \leq C_S^l \leq \min\{\sqrt{S} \frac{1+2\text{Lip}_\psi B_{\Theta}}{2(\text{Lip}_{\phi_1}\alpha + \text{Lip}_{\phi_2}\beta)}, S\}$ ($l = 1, \dots, L$) such that for any $\delta \in (0, 1)$, with probability at least $1 - \delta$, every $x^L(\cdot; \Theta_L^{\text{total}}) \in \mathcal{F}^L$ satisfies*

$$(3.4) \quad \begin{aligned} GE_{\mathcal{S}}(x^L(\cdot; \Theta_L^{\text{total}})) &\leq 2\sqrt{2}nB_{\kappa}B_{\Theta} \frac{M(T, \text{Lip}_\psi, n_d, B_{\text{in}}, B_{\Theta})}{\sqrt{S}} + 4B_\ell \sqrt{\frac{2\log(4/\delta)}{S}} \\ &\quad + (-2\sqrt{2})nB_{\kappa}B_{\Theta} \frac{(\text{Lip}_{\phi_1}\alpha + \text{Lip}_{\phi_2}\beta) \exp(T\text{Lip}_\psi B_{\Theta}^2)}{S} \tau_L \sum_{l=1}^L C_S^l, \end{aligned}$$

where $M(T, \text{Lip}_\psi, n_d, B_{\text{in}}, B_{\Theta}) = \left(\text{Lip}_\psi B_{\text{in}} \sqrt{2\log(2n_d)} + 1 + T(1 + 2\text{Lip}_\psi B_{\Theta}) \right) \exp(2T\text{Lip}_\psi B_{\Theta}^2)$, B_{κ}, B_ℓ are constants dependent on $T, B_{\text{in}}, B_{\Theta}, \text{Lip}_\psi$ and independent of L .

Proof. The proof is given in Section 4.2. □

Remark 3.6. **The bound in (3.4) consists of a leading positive term that is independent of the network depth L , together with a non-positive depth-dependent structural term of the form**

$$-2\sqrt{2}nB_{\kappa}B_{\Theta} \frac{(\text{Lip}_{\phi_1}\alpha + \text{Lip}_{\phi_2}\beta) \exp(T\text{Lip}_\psi B_{\Theta}^2)}{S} \tau_L \sum_{l=1}^L C_S^l.$$

Although this structural term appears with a negative sign in (3.4), the resulting right-hand side remains non-negative. This is guaranteed by the construction of the constants C_S^l , $1 \leq l \leq L$, as shown in the proof of Theorem 3.5. If we further discard the minus term, one immediately obtains a depth-uniform upper bound.

Remark 3.7. The non-positive structural term in the generalization bound reflects a structural effect induced by the activation function. This term depends on several activation-related constants, including $\text{Lip}_{\phi_1}, \text{Lip}_{\phi_2}, \alpha$, and β . Note that the associated data-dependent quantities C_S^l are introduced in an existential manner. Therefore, it is difficult to characterize explicitly for realistic network architectures and data distributions. Even for simplified settings, their precise values can be nontrivial to compute (see Example 3.1). **As a result, it is generally difficult to quantitatively compare the tightness of different generalization bounds for the same model, or to derive explicit design rules for activation parameters.** Nevertheless, this negative structural term theoretically reveals the potential role of activation function structure

in improving generalization. From a practical perspective, this suggests that learning activation parameters (such as α and β) may enable the network to discover activation configurations that yield improved generalization performance. We will further explore this phenomenon empirically in the experimental section.

Remark 3.8. The bound in (3.4) is independent of the network width and hidden dimensions, which is consistent with practical applications and aligns with [12]. Unlike [12], where the bound exhibits an explicit dependence on the network depth, our result can be further controlled by an explicit depth-independent upper bound (see Remark 3.6). Moreover, it remains unclear whether the path-norm framework in [12] extends to the continuous-time ResNet arising in the deep-layer limit. In contrast, our analysis admits a natural asymptotic interpretation with respect to depth, suggesting that discretizations of ODE-based architectures yield consistent discrete networks and lead to generalization bounds for continuous-time ResNets, as developed below. The bound also attains the optimal $O(1/\sqrt{S})$ rate established in prior works on discrete-time ResNets [31, 21, 12], which is sharper than the $O(1/\sqrt[4]{S})$ bound obtained in [34] in the discrete-time setting. The exponential factor depends only on the terminal time T , the Lipschitz constant of the activation function, and the parameter norm bound. Such exponential-in-time dependence is standard in dynamical system and neural ODE analyses, typically arising from Grönwall-type estimates [34, 6, 20]. These findings highlight a novel interplay between continuous-time neural networks, architectural stability, and generalization behavior, setting the stage for the deep-layer limit results developed in the next theorem.

THEOREM 3.9. (*Generalization error for continuous-time ResNets*) Assume assumptions (A_1) - (A_4) hold. Let the activation function $\psi \in \mathcal{A}(\mathbb{R})$ with $\phi_1, \phi_2 \in \Gamma(\mathbb{R})$ and $\alpha, \beta > 0$. Then there is a constant C_S dependent on \mathcal{S} , $0 \leq C_S \leq \min\{\sqrt{S} \frac{1+2\text{Lip}_\psi B_\Theta}{2(\text{Lip}_{\phi_1}\alpha + \text{Lip}_{\phi_2}\beta)}, S\}$ such that for any $\delta \in (0, 1)$, with probability at least $1 - \delta$, every $\mathbf{x}(T; \cdot; \Theta^{\text{total}}) \in \mathcal{F}^T$ satisfies

$$(3.5) \quad \begin{aligned} GE_{\mathcal{S}}(\mathbf{x}(T; \cdot; \Theta^{\text{total}})) &\leq 2\sqrt{2}nB_\kappa B_\Theta \frac{M(T, \text{Lip}_\psi, n_d, B_{\text{in}}, B_\Theta)}{\sqrt{S}} + 4B_\ell \sqrt{\frac{2\log(4/\delta)}{S}}, \\ &\quad - \frac{(\text{Lip}_{\phi_1}\alpha + \text{Lip}_{\phi_2}\beta) \exp(T\text{Lip}_\psi B_\Theta^2)T}{S} C_S, \end{aligned}$$

where $M(T, \text{Lip}_\psi, n_d, B_{\text{in}}, B_\Theta) = \left(\text{Lip}_\psi B_{\text{in}} \sqrt{2\log(2n_d)} + 1 + T(1 + 2\text{Lip}_\psi B_\Theta)\right) \exp(2T\text{Lip}_\psi B_\Theta^2)$, B_κ, B_ℓ are constants dependent on $T, B_{\text{in}}, B_\Theta, \text{Lip}_\psi$ and independent of L .

Proof. The proof is given in Section 4.3. □

Remark 3.10. The bound in (3.5) admits the same structural decomposition as its discrete-time counterpart: it consists of a leading term of order $O(1/\sqrt{S})$, add a data-dependent but non-positive structure term. In particular, the bound remains well-defined and non-negative. This generalization error for continuous-time ResNets is uniformly controlled over the time horizon and does not dependent on layer number L . As a special case, when the learnable parameters are constant in time, our bound directly yields an $O(1/\sqrt{S})$ generalization estimate for neural ODEs [8]. Combined with the discrete-time result in (3.4), this analysis shows that the generalization performance of ResNets remains uniformly bounded as the depth tends to infinity, providing theoretical support for the asymptotic consistency of deep residual architectures.

Remark 3.11. For comparison, Marion [34] established a generalization bound for a related continuous-time model under additional regularity assumptions on the time dependence of the

parameters, obtaining a rate of order $O(S^{-1/4})$. Closely related bounds of the same order were later derived for neural controlled differential equations using Lipschitz-based complexity arguments [6]. By contrast, our result is obtained under more general parameter assumptions and achieves an $O(1/\sqrt{S})$ rate. More recently, Hanson and Raginsky [20] derived an $O(1/\sqrt{S})$ generalization bound for neural ODEs via a Chen-Fliess series representation. While their analysis provides sharp sample complexity guarantees for continuous-depth models, it does not address the relationship between discrete-time ResNets and their continuous-time limits. Our result, instead, yields consistent $O(1/\sqrt{S})$ bounds for both discrete- and continuous-time settings within a unified framework.

4. Proofs. In this section, we present detailed proofs for the main results. We start with the proof for Proposition 3.2.

4.1. Proof of Proposition 3.2.

Proof. (Proof of Proposition 3.2) The proof follows the chaining method framework [47, 44] and is divided into three steps. The key idea is to carefully track how the piecewise structure of the activation function interacts with the Rademacher variables, allowing us to extract a negative correction term beyond the standard Lipschitz-based bound.

Step 1: We use the chaining method to decouple $\varepsilon_{(S)}$. Let $\boldsymbol{\varepsilon}_s := \{\varepsilon_{(1)}, \dots, \varepsilon_{(s)}\}$ for $1 \leq s \leq S$, and $R := \mathbb{E}_{\boldsymbol{\varepsilon}_S} \sup_{g \in \mathcal{G}} \left[\sum_{s=1}^S \varepsilon_{(s)} \psi(g(z_{(s)})) \right]$. Since $\varepsilon_{(s)}$ ($1 \leq s \leq S$) are independently and uniformly distributed over $\{-1, 1\}$, we have

$$\begin{aligned}
 (4.1) \quad R &= \frac{1}{2} \mathbb{E}_{\boldsymbol{\varepsilon}_{S-1}} \sup_{g \in \mathcal{G}} \left[\psi(g(z_{(S)})) + \sum_{s=1}^{S-1} \varepsilon_{(s)} \psi(g(z_{(s)})) \right] \\
 &\quad + \frac{1}{2} \mathbb{E}_{\boldsymbol{\varepsilon}_{S-1}} \sup_{g \in \mathcal{G}} \left[-\psi(g(z_{(S)})) + \sum_{s=1}^{S-1} \varepsilon_{(s)} \psi(g(z_{(s)})) \right] \\
 &= \frac{1}{2} \mathbb{E}_{\boldsymbol{\varepsilon}_{S-1}} \sup_{g, \hat{g} \in \mathcal{G}} \left\{ [\psi(g(z_{(S)})) - \psi(\hat{g}(z_{(S)}))] + \sum_{s=1}^{S-1} \varepsilon_{(s)} [\psi(g(z_{(s)})) + \psi(\hat{g}(z_{(s)}))] \right\}.
 \end{aligned}$$

Let $u_{\boldsymbol{\varepsilon}_s}(g, \hat{g}) := \sum_{i=1}^s \varepsilon_{(i)} [\psi(g(z_{(i)})) + \psi(\hat{g}(z_{(i)}))]$ for $s \geq 1$ and $u_0(g, \hat{g}) := 0$. We observe that $u_{\boldsymbol{\varepsilon}_s}(g, \hat{g})$ is symmetric, i.e., $u_{\boldsymbol{\varepsilon}_s}(g, \hat{g}) = u_{\boldsymbol{\varepsilon}_s}(\hat{g}, g)$.

Step 2: We estimate the first term in the right-hand side of Eq. (4.1). Because the activation functions in $\mathcal{A}(\mathbb{R})$ have a piecewise structure in the regions $(-\infty, -\beta)$, $[-\beta, \alpha]$, and $(\alpha, +\infty)$, we divide \mathcal{G} into three categories

$$\begin{cases}
 \mathcal{G}^{-1} = \{g \in \mathcal{G} : g(z_{(S)}) < -\beta\}, \\
 \mathcal{G}^0 = \{g \in \mathcal{G} : -\beta \leq g(z_{(S)}) \leq \alpha\}, \\
 \mathcal{G}^1 = \{g \in \mathcal{G} : g(z_{(S)}) > \alpha\}.
 \end{cases}$$

Define $\gamma_{a,b} = \sup_{g \in \mathcal{G}^a, \hat{g} \in \mathcal{G}^b} \left\{ [\psi(g(z_{(S)})) - \psi(\hat{g}(z_{(S)}))] + u_{\boldsymbol{\varepsilon}_{S-1}}(g, \hat{g}) \right\}$, where $a, b \in \{-1, 0, 1\}$. Next, we estimate $\gamma_{a,b}$.

- (i) For $(g, \hat{g}) \in \mathcal{G}^a \times \mathcal{G}^b$ with $a = b$ (i.e., $(a, b) = (-1, -1)$, $(a, b) = (0, 0)$, or $(a, b) = (1, 1)$), we have $\psi(g(z_{(S)})) - \psi(\hat{g}(z_{(S)})) \leq \text{Lip}_\psi \cdot |g(z_{(S)}) - \hat{g}(z_{(S)})|$, since ψ is Lip_ψ -Lipschitz continuous.

Therefore,

$$\begin{aligned}\gamma_{a,b} &\leq \sup_{g \in \mathcal{G}^a, \hat{g} \in \mathcal{G}^b} \left\{ \text{Lip}_\psi |g(z(S)) - \hat{g}(z(S))| + u_{\boldsymbol{\varepsilon}_{S-1}}(g, \hat{g}) \right\} \\ &= \sup_{g \in \mathcal{G}^a, \hat{g} \in \mathcal{G}^b} \left\{ \text{Lip}_\psi (g(z(S)) - \hat{g}(z(S))) + u_{\boldsymbol{\varepsilon}_{S-1}}(g, \hat{g}) \right\},\end{aligned}$$

where the last equality is due to the symmetric of $u_{\boldsymbol{\varepsilon}_{S-1}}$.

(ii) For $(g, \hat{g}) \in \mathcal{G}^a \times \mathcal{G}^b$ with $a - b = 1$ (i.e., $(a, b) = (0, -1)$ or $(a, b) = (1, 0)$), we obtain

$$\psi(g(z(S))) - \psi(\hat{g}(z(S))) \leq \text{Lip}_\psi |g(z(S)) - \hat{g}(z(S))| = \text{Lip}_\psi (g(z(S)) - \hat{g}(z(S))).$$

Therefore,

$$\gamma_{a,b} \leq \sup_{g \in \mathcal{G}^a, \hat{g} \in \mathcal{G}^b} \left\{ \text{Lip}_\psi (g(z(S)) - \hat{g}(z(S))) + u_{\boldsymbol{\varepsilon}_{S-1}}(g, \hat{g}) \right\}.$$

(iii) For $(g, \hat{g}) \in \mathcal{G}^a \times \mathcal{G}^b$ with $a - b = 2$ (i.e., $(a, b) = (1, -1)$), we note that $-\hat{g}(z(S)) - \beta > 0$, and

$$\begin{aligned}\psi(g(z(S))) - \psi(\hat{g}(z(S))) &= \phi_1(g(z(S)) - \alpha) + \phi_2(-\hat{g}(z(S)) - \beta) \\ &\leq \text{Lip}_{\phi_1}(g(z(S)) - \alpha) + \text{Lip}_{\phi_2}(-\hat{g}(z(S)) - \beta) \\ &\leq \text{Lip}_\psi (g(z(S)) - \hat{g}(z(S))) - (\text{Lip}_{\phi_1} \alpha + \text{Lip}_{\phi_2} \beta),\end{aligned}$$

where the second inequality uses $\text{Lip}_{\phi_1}, \text{Lip}_{\phi_2} \leq \text{Lip}_\psi$. Therefore,

$$\gamma_{a,b} \leq \sup_{g \in \mathcal{G}^a, \hat{g} \in \mathcal{G}^b} \left\{ \text{Lip}_\psi (g(z(S)) - \hat{g}(z(S))) + u_{\boldsymbol{\varepsilon}_{S-1}}(g, \hat{g}) - (\text{Lip}_{\phi_1} \alpha + \text{Lip}_{\phi_2} \beta) \right\}.$$

(iv) For $(g, \hat{g}) \in \mathcal{G}^a \times \mathcal{G}^b$ with $a - b < 0$ (i.e., $(a, b) = (-1, 0)$ or $(a, b) = (0, 1)$ or $(a, b) = (-1, 1)$), we have

$$\psi(g(z(S))) - \psi(\hat{g}(z(S))) \leq \text{Lip}_\psi |g(z(S)) - \hat{g}(z(S))| = \text{Lip}_\psi (\hat{g}(z(S)) - g(z(S))).$$

Therefore,

$$\begin{aligned}\gamma_{a,b} &\leq \sup_{g \in \mathcal{G}^a, \hat{g} \in \mathcal{G}^b} \left\{ \text{Lip}_\psi (\hat{g}(z(S)) - g(z(S))) + u_{\boldsymbol{\varepsilon}_{S-1}}(g, \hat{g}) \right\} \\ &= \sup_{g \in \mathcal{G}^a, \hat{g} \in \mathcal{G}^b} \left\{ \text{Lip}_\psi (\hat{g}(z(S)) - g(z(S))) + u_{\boldsymbol{\varepsilon}_{S-1}}(\hat{g}, g) \right\} = \gamma_{b,a}.\end{aligned}$$

Combining the above discussions, we obtain

$$(4.2) \quad \begin{aligned} &\max_{a,b \in \{-1,0,1\}} \gamma_{a,b} \\ &\leq \sup_{g, \hat{g} \in \mathcal{G}} \left\{ \text{Lip}_\psi (g(z(S)) - \hat{g}(z(S))) + u_{\boldsymbol{\varepsilon}_{S-1}}(g, \hat{g}) - (\text{Lip}_{\phi_1} \alpha + \text{Lip}_{\phi_2} \beta) \cdot \mathbf{1}_{\mathcal{G}^1 \times \mathcal{G}^{-1}}((g, \hat{g})) \right\},\end{aligned}$$

where

$$\mathbf{1}_{\mathcal{G}^1 \times \mathcal{G}^{-1}}(g, \hat{g}) = \begin{cases} 1, & (g, \hat{g}) \in \mathcal{G}^1 \times \mathcal{G}^{-1}, \\ 0, & (g, \hat{g}) \notin \mathcal{G}^1 \times \mathcal{G}^{-1}. \end{cases}$$

The indicator term explicitly encodes the frequency with which function pairs fall into the extreme regions of the activation, quantifying how often the negative structural contribution is activated across the sample.

Step 3: We now aggregate the negative contributions accumulated over all Rademacher configurations, yielding a data-dependent constant in Eq. (3.1) that captures the overall strength of the structural correction. For any $\eta > 0$ and any given $\boldsymbol{\varepsilon}_S \setminus \varepsilon_{(S)} \in \{-1, 1\}^{S-1}$, there exist functions $g_{\boldsymbol{\varepsilon}_S \setminus \varepsilon_{(S)}}, \hat{g}_{\boldsymbol{\varepsilon}_S \setminus \varepsilon_{(S)}}^* \in \mathcal{G}$ such that

$$(4.3) \quad \begin{aligned} & \sup_{g, \hat{g} \in \mathcal{G}} \left\{ \text{Lip}_\psi(g(z_{(S)}) - \hat{g}(z_{(S)})) + u_{\boldsymbol{\varepsilon}_{S-1}}(g, \hat{g}) - (\text{Lip}_{\phi_1} \alpha + \text{Lip}_{\phi_2} \beta) \cdot \mathbf{1}_{\mathcal{G}^1 \times \mathcal{G}^{-1}}(g, \hat{g}) \right\} \\ & \leq \text{Lip}_\psi(g_{\boldsymbol{\varepsilon}_S \setminus \varepsilon_{(S)}}^*(z_{(S)}) - \hat{g}_{\boldsymbol{\varepsilon}_S \setminus \varepsilon_{(S)}}^*(z_{(S)})) + u_{\boldsymbol{\varepsilon}_{S-1}}(g_{\boldsymbol{\varepsilon}_S \setminus \varepsilon_{(S)}}^*, \hat{g}_{\boldsymbol{\varepsilon}_S \setminus \varepsilon_{(S)}}^*) \\ & \quad - (\text{Lip}_{\phi_1} \alpha + \text{Lip}_{\phi_2} \beta) \mathbf{1}_{\mathcal{G}^1 \times \mathcal{G}^{-1}}(g_{\boldsymbol{\varepsilon}_S \setminus \varepsilon_{(S)}}^*, \hat{g}_{\boldsymbol{\varepsilon}_S \setminus \varepsilon_{(S)}}^*) + \eta/S. \end{aligned}$$

By combining Eqs. (4.1)–(4.3), we get

$$\begin{aligned} R & \leq \frac{1}{2} \mathbb{E}_{\boldsymbol{\varepsilon}_{S-1}} \sup_{g, \hat{g} \in \mathcal{G}} \left\{ \text{Lip}_\psi(g(z_{(S)}) - \hat{g}(z_{(S)})) + u_{\boldsymbol{\varepsilon}_{S-1}}(g, \hat{g}) \right\} \\ & \quad - \frac{\text{Lip}_{\phi_1} \alpha + \text{Lip}_{\phi_2} \beta}{2^{S-1}} \cdot \sum_{\boldsymbol{\varepsilon}_S \setminus \varepsilon_{(S)} \in \{-1, 1\}^{S-1}} \mathbf{1}_{\mathcal{G}^1 \times \mathcal{G}^{-1}}(g_{\boldsymbol{\varepsilon}_S \setminus \varepsilon_{(S)}}^*, \hat{g}_{\boldsymbol{\varepsilon}_S \setminus \varepsilon_{(S)}}^*) + \eta/S \\ & = \mathbb{E}_{\boldsymbol{\varepsilon}_S} \sup_{g \in \mathcal{G}} \left\{ \varepsilon_{(S)} \text{Lip}_\psi g(z_{(S)}) + \sum_{s=1}^{S-1} \varepsilon_{(s)} \psi(g(z_{(s)})) \right\} \\ & \quad - \frac{\text{Lip}_{\phi_1} \alpha + \text{Lip}_{\phi_2} \beta}{2^{S-1}} \cdot \sum_{\boldsymbol{\varepsilon}_S \setminus \varepsilon_{(S)} \in \{-1, 1\}^{S-1}} \mathbf{1}_{\mathcal{G}^1 \times \mathcal{G}^{-1}}(g_{\boldsymbol{\varepsilon}_S \setminus \varepsilon_{(S)}}^*, \hat{g}_{\boldsymbol{\varepsilon}_S \setminus \varepsilon_{(S)}}^*) + \eta/S. \end{aligned}$$

It follows by iterating the above process for $S - 1$ more steps (i.e., for $s \in \{1, \dots, S - 1\}$) that

$$\begin{aligned} R & \leq \text{Lip}_\psi \cdot \mathbb{E}_{\boldsymbol{\varepsilon}_S} \sup_{g \in \mathcal{G}} \left\{ \sum_{s=1}^S \varepsilon_{(s)} g(z_{(s)}) \right\} \\ & \quad - \frac{\text{Lip}_{\phi_1} \alpha + \text{Lip}_{\phi_2} \beta}{2^{S-1}} \cdot \sum_{s=1}^S \sum_{\boldsymbol{\varepsilon}_S \setminus \varepsilon_{(s)} \in \{-1, 1\}^{S-1}} \mathbf{1}_{\mathcal{G}^1 \times \mathcal{G}^{-1}}(g_{\boldsymbol{\varepsilon}_S \setminus \varepsilon_{(s)}}^*, \hat{g}_{\boldsymbol{\varepsilon}_S \setminus \varepsilon_{(s)}}^*) + \eta, \end{aligned}$$

where $g_{\boldsymbol{\varepsilon}_S \setminus \varepsilon_{(s)}}^*, \hat{g}_{\boldsymbol{\varepsilon}_S \setminus \varepsilon_{(s)}}^* \in \mathcal{G}$. Hence,

$$\mathcal{R}_{\mathcal{Z}}(\psi \circ \mathcal{G}) \leq \text{Lip}_\psi \cdot \mathcal{R}_{\mathcal{Z}}(\mathcal{G}) - \frac{(\text{Lip}_{\phi_1} \alpha + \text{Lip}_{\phi_2} \beta)}{S} C_{\mathcal{Z}}(\eta) + \eta/S,$$

where $C_{\mathcal{Z}}(\eta) = \frac{1}{2^{S-1}} \sum_{s=1}^S \sum_{\boldsymbol{\varepsilon}_S \setminus \varepsilon_{(s)} \in \{-1, 1\}^{S-1}} \mathbf{1}_{\mathcal{G}^1 \times \mathcal{G}^{-1}}(g_{\boldsymbol{\varepsilon}_S \setminus \varepsilon_{(s)}}^*, \hat{g}_{\boldsymbol{\varepsilon}_S \setminus \varepsilon_{(s)}}^*)$ is dependent on \mathcal{Z} . Taking the limit as $\eta \rightarrow 0$, we obtain (along a subsequence) that $C_{\mathcal{Z}}(\eta) \rightarrow C_{\mathcal{Z}}$ for some $0 \leq C_{\mathcal{Z}} \leq S$. Thus,

$$\mathcal{R}_{\mathcal{Z}}(\psi \circ \mathcal{G}) \leq \text{Lip}_\psi \cdot \mathcal{R}_{\mathcal{Z}}(\mathcal{G}) - \frac{\text{Lip}_{\phi_1} \alpha + \text{Lip}_{\phi_2} \beta}{S} C_{\mathcal{Z}}.$$

Since the Rademacher complexity is nonnegative, we get $C_{\mathcal{Z}} \leq \frac{\text{Lip}_\psi S}{\text{Lip}_{\phi_1} \alpha + \text{Lip}_{\phi_2} \beta} \mathcal{R}_{\mathcal{Z}}(\mathcal{G})$, and thus complete the proof. \square

4.2. Proof of Theorem 3.5. In this subsection, we give a detailed proof for Theorem 3.5. The following lemma provides the boundedness of state variables.

LEMMA 4.1. *Assume assumptions (A₁) – (A₃) hold. Given any learnable parameters $\Theta_L^{\text{total}} \in \Omega_{\Theta^{\text{total}}}$, $\Theta^{\text{total}} \in \Omega_{\Theta^{\text{total}}}$ and input $\mathbf{d} \in \mathbb{R}^{n_d}$ such that $\|\mathbf{d}\|_\infty \leq B_{\text{in}}$. Then the state variables $\{\mathbf{x}^l(\mathbf{d}; \Theta_L^{\text{total}})\}_{l=0}^L$ of discrete-time ResNet (2.1) and $\{\mathbf{x}(t; \mathbf{d}; \Theta^{\text{total}}) : 0 \leq t \leq T\}$ of continuous-time ResNet (2.5) exist uniquely and satisfy*

$$\begin{aligned} \|\mathbf{x}^l(\mathbf{d}; \Theta_L^{\text{total}})\|_\infty &\leq \left[\text{Lip}_\psi B_{\Theta} (B_{\text{in}} + 1) + \tau_L l (\text{Lip}_\psi B_{\Theta}^2 + B_{\Theta}) \right] \exp(\tau_L l \text{Lip}_\psi B_{\Theta}^2) =: B_{\text{out}}^l, \\ \|\mathbf{x}(t; \mathbf{d}; \Theta^{\text{total}})\|_\infty &\leq \left[\text{Lip}_\psi B_{\Theta} (B_{\text{in}} + 1) + t (\text{Lip}_\psi B_{\Theta}^2 + B_{\Theta}) \right] \exp(t \text{Lip}_\psi B_{\Theta}^2) =: B_{\text{out}}^t, \end{aligned}$$

respectively. Moreover, let $B_{\text{out}} = \left[\text{Lip}_\psi B_{\Theta} (B_{\text{in}} + 1) + T (\text{Lip}_\psi B_{\Theta}^2 + B_{\Theta}) \right] \exp(T \text{Lip}_\psi B_{\Theta}^2)$. We then have

$$\max\left\{ \max_{0 \leq l \leq L} \|\mathbf{x}^l(\mathbf{d}; \Theta_L^{\text{total}})\|_\infty, \max_{0 \leq t \leq T} \|\mathbf{x}(t; \mathbf{d}; \Theta^{\text{total}})\|_\infty \right\} \leq B_{\text{out}}.$$

Proof. The proof is standard and is supplied in supplementary materials. \square

The uniform bound B_{out} for the discrete- and continuous-time states implies a uniform bound B_ℓ and a uniform local Lipschitz coefficient B_κ for the loss function ℓ used in both discrete- and continuous-time settings. These constants depend only on $T, B_{\text{in}}, B_{\Theta}, \text{Lip}_\psi$, and will be used in proving Theorems 3.5 and 3.9. The next lemma establishes an equivalence property of hypothesis sets \mathcal{F}_i^l ($1 \leq i \leq n$) under assumptions (A₁) (A₂), which plays a key role in proving Theorem 3.5.

LEMMA 4.2. *Let assumptions (A₁)-(A₂) hold. For any layer $0 \leq l \leq L$, the hypothesis sets \mathcal{F}_i^l ($1 \leq i \leq n$) defined in (2.4) satisfy $\mathcal{F}_{i_1}^l = \mathcal{F}_{i_2}^l, i_1, i_2 \in \{1, \dots, n\}$.*

Proof. Let $\mathbf{P}_{(ij)}$ be the $n \times n$ permutation matrix swapping coordinates i and j , i.e., $\mathbf{P}_{(ij)} := \mathbf{I} + (\mathbf{e}_{(i)} - \mathbf{e}_{(j)})(\mathbf{e}_{(j)} - \mathbf{e}_{(i)})^\top$, where \mathbf{e}_i represents the i -th standard basis vector in an n -dimensional space, with 1 at the i -th position and 0 elsewhere, $\mathbf{I} \in \mathbb{R}^{n \times n}$ is the identity matrix. Denote $\Theta_l := (\Theta_l^0, \Theta_l^1, \dots, \Theta_l^{l-1}) \in \mathcal{E}^l, \Theta_l^{\text{total}} := (\Theta^{\text{pre}}, \Theta_l) \in \mathcal{E}^{\text{pre}} \times \mathcal{E}^l$. We show by induction on l that, for each choice of parameters $\Theta_l^{\text{total}} \in \Omega_{\Theta^{\text{total}}}$ and indices $i_1, i_2 \in \{1, \dots, n\}$, there is a modified parameter $\tilde{\Theta}_l^{\text{total}} \in \Omega_{\Theta^{\text{total}}}$ such that

$$\mathbf{x}^l(\mathbf{d}; \tilde{\Theta}_l^{\text{total}}) = \mathbf{P}_{(i_1 i_2)} \mathbf{x}^l(\mathbf{d}; \Theta_l^{\text{total}}).$$

Since $\mathbf{P}_{(i_1 i_2)}^2 = \mathbf{I}$, this establishes a bijection between the i_1 -th and i_2 -th output functions, hence $\mathcal{F}_{i_1}^l = \mathcal{F}_{i_2}^l$.

For the preprocessing layer, if $\Theta^{\text{pre}} = (\mathbf{U}, \mathbf{a}) \in \mathcal{E}^{\text{pre}}$ and $i_1, i_2 \in \{1, \dots, n\}$, let $\tilde{\Theta}^{\text{pre}} = (\mathbf{P}_{(i_1 i_2)} \mathbf{U}, \mathbf{P}_{(i_1 i_2)} \mathbf{a}) \in \mathcal{E}^{\text{pre}}$. Then it is easy to see

$$\mathbf{x}^0(\mathbf{d}; \tilde{\Theta}^{\text{pre}}) = \psi \circ (\mathbf{P}_{(i_1 i_2)} \mathbf{U} \mathbf{d} + \mathbf{P}_{(i_1 i_2)} \mathbf{a}) = \mathbf{P}_{(i_1 i_2)} \psi \circ (\mathbf{U} \mathbf{d} + \mathbf{a}) = \mathbf{P}_{(i_1 i_2)} \mathbf{x}^0(\mathbf{d}; \Theta^{\text{pre}}), \quad \forall \mathbf{d} \in \mathbb{R}^{n_d},$$

by the element-wise action of ψ . For $l = 0$ and given parameter $\Theta_0^{\text{total}} = ((\mathbf{U}, \mathbf{a}), (\mathbf{V}^0, \mathbf{W}^0, \mathbf{b}^0, \mathbf{a}^0)) \in \Theta_0^{\text{total}}$ and $i_1, i_2 \in \{1, \dots, n\}$, let $\tilde{\Theta}_0^{\text{total}} = ((\tilde{\mathbf{U}}, \tilde{\mathbf{a}}), (\tilde{\mathbf{V}}^0, \tilde{\mathbf{W}}^0, \mathbf{b}^0, \tilde{\mathbf{c}}^0)) \in \Omega_{\Theta_0^{\text{total}}}$, where

$$\tilde{\mathbf{U}} = \mathbf{P}_{(i_1 i_2)} \mathbf{U}, \quad \tilde{\mathbf{a}} = \mathbf{P}_{(i_1 i_2)} \mathbf{a}, \quad \tilde{\mathbf{V}}^0 = \mathbf{V}^0 \mathbf{P}_{(i_1 i_2)}, \quad \tilde{\mathbf{W}}^0 = \mathbf{P}_{(i_1 i_2)} \mathbf{W}^0, \quad \tilde{\mathbf{c}}^0 = \mathbf{P}_{(i_1 i_2)} \mathbf{c}^0.$$

Then we have

$$\mathbf{x}^0(\mathbf{d}; \tilde{\Theta}^{\text{pre}}) = \psi \circ (\mathbf{P}_{(i_1 i_2)} \mathbf{U} \mathbf{d} + \mathbf{P}_{(i_1 i_2)} \mathbf{a}) = \mathbf{P}_{(i_1 i_2)} \psi \circ (\mathbf{U} \mathbf{d} + \mathbf{a}) = \mathbf{P}_{(i_1 i_2)} \mathbf{x}^0(\mathbf{d}; \Theta^{\text{pre}})$$

and

$$\begin{aligned} \mathbf{x}_{i_1}^1(\mathbf{d}; \tilde{\Theta}_0^{\text{total}}) &= \mathbf{x}_{i_1}^0(\mathbf{d}; \tilde{\Theta}^{\text{pre}}) + \tau_L \left(\tilde{\mathbf{W}}_{i_1, \cdot}^0 \psi \circ (\tilde{\mathbf{V}}^0 \mathbf{x}^0(\mathbf{d}; \tilde{\Theta}^{\text{pre}}) + \mathbf{b}^0) + \tilde{\mathbf{c}}_{i_1}^0 \right) \\ &= \mathbf{x}_{i_2}^0(\mathbf{d}; \Theta^{\text{pre}}) + \tau_L \left(\mathbf{W}_{i_2, \cdot}^0 \psi \circ (\mathbf{V}^0 \mathbf{x}^0(\mathbf{d}; \Theta^{\text{pre}}) + \mathbf{b}^0) + \mathbf{c}_{i_2}^0 \right) \\ &= \mathbf{x}_{i_2}^1(\mathbf{d}; \Theta_0^{\text{total}}), \quad \forall \mathbf{d} \in \mathbb{R}^{n_d}, \end{aligned}$$

owing to the definition of \mathcal{F}_i^l (for $l = 0$) in (2.4), $\mathbf{P}_{(i_1 i_2)} \mathbf{P}_{(i_1 i_2)} = \mathbf{I}$ and the element-wise action of ψ . Through a similar procedure as described above, we can derive that $\mathbf{x}_{i_2}^1(\mathbf{d}; \tilde{\Theta}_0^{\text{total}}) = \mathbf{x}_{i_1}^1(\mathbf{d}; \Theta_0^{\text{total}})$ and $\mathbf{x}_i^1(\mathbf{d}; \tilde{\Theta}_0^{\text{total}}) = \mathbf{x}_i^1(\mathbf{d}; \Theta_0^{\text{total}})$, $i \neq i_1, i_2$, i.e., $\mathbf{x}^1(\mathbf{d}; \tilde{\Theta}_0^{\text{total}}) = \mathbf{P}_{(i_1 i_2)} \mathbf{x}^1(\mathbf{d}; \Theta_0^{\text{total}})$.

Suppose the claim holds for layer $l \leq K$, where $K \geq 2$ and $K \in \mathbb{N}$. Given parameter $\Theta_{K+1}^{\text{total}} = (\Theta_{K+1}^{\text{pre}}, \Theta_{K+1}^0, \dots, \Theta_{K+1}^K) \in \Omega_{\Theta_{K+1}^{\text{total}}}$ and $i_1, i_2 \in \{1, \dots, n\}$. By the inductive hypothesis, we can find parameters $(\tilde{\Theta}_K^{\text{pre}}, \tilde{\Theta}_K^0, \dots, \tilde{\Theta}_K^{K-1}) \in \Omega_{\Theta_K^{\text{total}}}$ such that for $\tilde{\Theta}_{K+1}^{\text{total}} = (\tilde{\Theta}_K^{\text{pre}}, \tilde{\Theta}_K^0, \dots, \tilde{\Theta}_K^{K-1}, \tilde{\Theta}_{K+1}^K)$ $= (\tilde{\Theta}_{K+1}^{\text{pre}}, \tilde{\Theta}_{K+1}^0, \dots, \tilde{\Theta}_{K+1}^{K-1}, \tilde{\Theta}_{K+1}^K) \in \Omega_{\Theta_{K+1}^{\text{total}}}$, there is

$$\mathbf{x}^K(\mathbf{d}; \tilde{\Theta}_{K+1}^{\text{total}}) = \mathbf{P}_{(i_1 i_2)} \mathbf{x}^K(\mathbf{d}; \Theta_{K+1}^{\text{total}}).$$

Let parameter $\tilde{\Theta}_{K+1}^K = (\tilde{\mathbf{V}}^K, \tilde{\mathbf{W}}^K, \mathbf{b}^K, \tilde{\mathbf{c}}^K)$, where $\tilde{\mathbf{V}}^K = \mathbf{V}^K \mathbf{P}_{(i_1 i_2)}$, $\tilde{\mathbf{W}}^K = \mathbf{P}_{(i_1 i_2)} \mathbf{W}^K$, $\tilde{\mathbf{c}}^K = \mathbf{P}_{(i_1 i_2)} \mathbf{c}^K$. We therefore obtain

$$\begin{aligned} \mathbf{x}_{i_1}^{K+1}(\mathbf{d}; \tilde{\Theta}_{K+1}^{\text{total}}) &= \mathbf{x}_{i_1}^K(\mathbf{d}; \tilde{\Theta}_{K+1}^{\text{total}}) + \tau_L \left(\tilde{\mathbf{W}}_{i_1, \cdot}^K \psi \circ (\tilde{\mathbf{V}}^K \mathbf{x}^K(\mathbf{d}; \tilde{\Theta}_{K+1}^{\text{total}}) + \mathbf{b}^K) + \tilde{\mathbf{c}}_{i_1}^K \right) \\ &= \mathbf{x}_{i_2}^K(\mathbf{d}; \Theta_{K+1}^{\text{total}}) + \tau_L \left(\mathbf{W}_{i_2, \cdot}^K \psi \circ (\mathbf{V}^K \mathbf{x}^K(\mathbf{d}; \Theta_{K+1}^{\text{total}}) + \mathbf{b}^K) + \mathbf{c}_{i_2}^K \right) \\ &= \mathbf{x}_{i_2}^{K+1}(\mathbf{d}; \Theta_{K+1}^{\text{total}}), \end{aligned}$$

due to the definition of \mathcal{F}_i^l ($l = K+1$) in (2.4), $\mathbf{P}_{(i_1 i_2)} \mathbf{P}_{(i_1 i_2)} = \mathbf{I}$ and the element-wise action of ψ . Besides, we can similarly get $\mathbf{x}^{K+1}(\mathbf{d}; \tilde{\Theta}_{K+1}^{\text{total}}) = \mathbf{P}_{(i_1 i_2)} \mathbf{x}^{K+1}(\mathbf{d}; \Theta_{K+1}^{\text{total}})$. These complete the proof. \square

We now prove Theorem 3.5.

Proof. (Proof of Theorem 3.5) We divide the proof into three steps. The proof strategy is to first reduce the generalization gap to a Rademacher complexity estimate, and then carefully propagate this complexity through the residual layers, tracking both the standard Lipschitz growth and a layer-wise negative correction induced by the activation structure.

Step 1. We first establish the boundedness of the loss function, which allows us to apply the result in [42, Theorem 26.5] to derive an upper bound on the generalization gap via Rademacher complexity. By assumptions $(A_1) - (A_3)$ and Lemma 4.1, the sets of state variable $\mathcal{S}_{\text{state}}^L := \{\mathbf{x}^L(\mathbf{d}; \Theta_L^{\text{total}}) : \Theta_L^{\text{total}} \in \Omega_{\Theta_L^{\text{total}}}, (\mathbf{d}, \mathbf{g}) \sim \mathfrak{D}\}$, $L \geq 1$ are uniformly bounded by a constant B_{out} dependent on $T, B_{\text{in}}, B_{\Theta}, \text{Lip}_{\psi}$. Therefore, the sets $\{\ell(\mathbf{x}^L(\mathbf{d}; \Theta_L^{\text{total}}), \mathbf{g}) : \Theta_L^{\text{total}} \in \Omega_{\Theta_L^{\text{total}}}, (\mathbf{d}, \mathbf{g}) \sim \mathfrak{D}\}$, $L \geq 1$ are bounded by a constant B_{ℓ} dependent on $T, B_{\text{in}}, B_{\Theta}, \text{Lip}_{\psi}$ due to the continuity of loss function. Hence, for any $0 < \delta < 1$, with probability $1 - \delta$,

$$(4.4) \quad GE_S(\mathbf{x}^L(\cdot; \Theta_L^{\text{total}})) \leq 2\mathcal{R}_S(\ell \circ \mathcal{F}^L) + 4B_{\ell} \sqrt{\frac{2 \log(4/\delta)}{S}}, \quad \forall \mathbf{x}^L(\cdot; \Theta_L^{\text{total}}) \in \mathcal{F}^L,$$

due to [42, Theorem 26.5]. Here $\ell \circ \mathcal{F}^L = \{f(d, g) = \ell(x^L(d; \Theta_L^{\text{total}}), g) : x^L(\cdot; \Theta_L^{\text{total}}) \in \mathcal{F}^L\}$.

Step 2. We estimate the complexity $\mathcal{R}_S(\ell \circ \mathcal{F}^L)$. Here, we exploit the Lipschitz property of the loss with respect to the network output to reduce the vector-valued Rademacher complexity to a sum of scalar-valued ones, thereby decoupling the dependence across output coordinates.

By assumption (A₄) and the discussion in Step 1, the sets $\{\kappa(x, \tilde{x}, g) : x, \tilde{x} \in \mathcal{S}_{\text{state}}^L; (d, g) \sim \mathfrak{D}\}$, $L \geq 1$ are uniformly bounded by a constant B_κ dependent on $T, B_{\text{in}}, B_\Theta, \text{Lip}_\psi$. Hence, ℓ is B_κ -Lipschitz for the first argument in $\{(x^L(d; \Theta_L^{\text{total}}), g) : \Theta_L^{\text{total}} \in \Omega_{\Theta_L^{\text{total}}}, (d, g) \sim \mathfrak{D}\}$, and we have,

$$\begin{aligned}
\mathcal{R}_S(\ell \circ \mathcal{F}^L) &= \mathbb{E}_\epsilon \sup_{\ell \circ x^L(\cdot; \Theta_L^{\text{total}}) \in \ell \circ \mathcal{F}^L} \frac{1}{S} \sum_{s=1}^S \varepsilon_{(s)} \cdot \ell(x^L(d_{(s)}; \Theta_L^{\text{total}}), g_{(s)}) \\
&= \mathbb{E}_\epsilon \sup_{x^L(\cdot; \Theta_L^{\text{total}}) \in \mathcal{F}^L} \frac{1}{S} \sum_{s=1}^S \varepsilon_{(s)} \cdot \ell(x^L(d_{(s)}; \Theta_L^{\text{total}}), g_{(s)}) \\
&\leq \sqrt{2} B_\kappa \mathbb{E}_\epsilon \sup_{x_k^L(\cdot; \Theta_L^{\text{total}}) \in \mathcal{F}_k^L} \frac{1}{S} \sum_{s=1}^S \sum_{k=1}^n \epsilon_{(sk)} x_k^L(d_{(s)}; \Theta_L^{\text{total}}) \\
&\leq \sqrt{2} B_\kappa \sum_{k=1}^n \mathbb{E}_{\epsilon_{k,\cdot}} \sup_{x_k^L(\cdot; \Theta_L^{\text{total}}) \in \mathcal{F}_k^L} \frac{1}{S} \sum_{s=1}^S \epsilon_{(sk)} x_k^L(d_{(s)}; \Theta_L^{\text{total}}) \\
(4.5) \quad &= \sqrt{2} B_\kappa \sum_{k=1}^n \mathcal{R}_S(\mathcal{F}_k^L),
\end{aligned}$$

where $\epsilon_{k,\cdot} = \{\epsilon_{1k}, \dots, \epsilon_{Sk}\}$, the first inequality follows from [35, Corollary 1].

Step 3. We estimate the Rademacher complexity $\mathcal{R}_S(\mathcal{F}_k^L)$ for $1 \leq k \leq n$. This step is the core of the analysis.

By Lemma 4.2, it suffices to estimate $\mathcal{R}_S(\mathcal{F}_1^L)$. For simplicity, define

$$z^{l+1}(d; \Theta_L^{\text{total}}) = V^l x^l(d; \Theta_L^{\text{total}}) + b^l, 0 \leq l \leq L-1.$$

By Lemma 4.2 and its proof, we can see each component of $z^{l+1}(\cdot; \Theta_L^{\text{total}})$ (i.e., $z_k^{l+1}(\cdot; \Theta_L^{\text{total}})$, $1 \leq k \leq m$) is in the same function class

$$\mathcal{Z}^{l+1} := \left\{ v^\top x^l(\cdot; \Theta_L^{\text{total}}) + b \mid v \in \mathbb{R}^n, b \in \mathbb{R}, \max\{\|v\|_1, |b|\} \leq B_\Theta; x^l(\cdot; \Theta_L^{\text{total}}) \in \mathcal{F}^l \right\}.$$

Therefore, we can derive that

$$\begin{aligned}
\mathcal{R}_S(\mathcal{F}_1^{l+1}) &= \frac{1}{S} \mathbb{E}_\epsilon \sup_{x_1^{l+1}(\cdot; \Theta_L^{\text{total}}) \in \mathcal{F}_1^{l+1}} \sum_{s=1}^S \varepsilon_{(s)} x_1^{l+1}(d_{(s)}; \Theta_L^{\text{total}}) \\
&= \frac{1}{S} \mathbb{E}_\epsilon \sup_{\substack{x^l(\cdot; \Theta_L^{\text{total}}) \in \mathcal{F}^l \\ \max\{\|c_1^l\|, \|W_{1,\cdot}^l\|_1\} \leq B_\Theta, \\ \max\{\|V^l\|_\infty, \|b^l\|_\infty\} \leq B_\Theta}} \sum_{s=1}^S \varepsilon_{(s)} \left[x_1^l(d_{(s)}; \Theta_L^{\text{total}}) + \tau_L \left(W_{1,\cdot}^l \psi \circ (V^l x^l(d_{(s)}; \Theta_L^{\text{total}}) + b^l) + c_1^l \right) \right]
\end{aligned}$$

$$\begin{aligned}
&\leq \frac{1}{S} \mathbb{E}_\epsilon \sup_{\substack{x_1^l(\cdot; \Theta_L^{\text{total}}) \in \mathcal{F}_1^l, \\ \max\{|c_1^l|, \|W_{1,\cdot}^l\|_1\} \leq B_\Theta, \\ z^{l+1}(\cdot; \Theta_L^{\text{total}}) \in (\mathcal{Z}^{l+1})^m}} \sum_{s=1}^S \varepsilon_{(s)} \left[x_1^l(d_{(s)}; \Theta_L^{\text{total}}) + \tau_L \left(W_{1,\cdot}^l \psi \circ (z^{l+1}(d_{(s)}; \Theta_L^{\text{total}})) + c_1^l \right) \right] \\
&\leq \mathcal{R}_S(\mathcal{F}_1^l) + \tau_L \frac{B_\Theta}{\sqrt{S}} + \tau_L 2B_\Theta \frac{1}{S} \mathbb{E}_\epsilon \sup_{z^{l+1}(\cdot; \Theta_L^{\text{total}}) \in \mathcal{Z}^{l+1}} \sum_{s=1}^S \varepsilon_{(s)} \psi(z_1^{l+1}(d_{(s)}; \Theta_L^{\text{total}})) \\
&\leq \mathcal{R}_S(\mathcal{F}_1^l) + \tau_L \frac{B_\Theta}{\sqrt{S}} + \tau_L \text{Lip}_\psi 2B_\Theta \frac{1}{S} \mathbb{E}_\epsilon \sup_{\substack{x^l(\cdot; \Theta_L^{\text{total}}) \in \mathcal{F}^l, \\ \max\{\|V_{1,\cdot}^l\|_1, |b_1^l|\} \leq B_\Theta}} \sum_{s=1}^S \varepsilon_{(s)} \left[V_{1,\cdot}^l x^l(d_{(s)}; \Theta_L^{\text{total}}) + b_1^l \right] \\
&\quad - \tau_L \frac{2B_\Theta (\text{Lip}_{\phi_1} \alpha + \text{Lip}_{\phi_2} \beta)}{S} \bar{C}_S^{l+1} \\
&\leq \mathcal{R}_S(\mathcal{F}_1^l) + \tau_L \frac{B_\Theta}{\sqrt{S}} + \tau_L 2\text{Lip}_\psi B_\Theta \left(\frac{B_\Theta}{\sqrt{S}} + B_\Theta \mathcal{R}_S(\mathcal{F}_1^l) \right) - \tau_L \frac{2B_\Theta (\text{Lip}_{\phi_1} \alpha + \text{Lip}_{\phi_2} \beta)}{S} \bar{C}_S^{l+1} \\
&\leq \mathcal{R}_S(\mathcal{F}_1^l) + \tau_L 2\text{Lip}_\psi B_\Theta^2 \mathcal{R}_S(\mathcal{F}_1^l) + \max \left\{ \tau_L \frac{B_\Theta}{\sqrt{S}} \left(1 + 2\text{Lip}_\psi B_\Theta \right) - \tau_L 2B_\Theta \frac{(\text{Lip}_{\phi_1} \alpha + \text{Lip}_{\phi_2} \beta) \bar{C}_S^{l+1}}{S}, 0 \right\},
\end{aligned}$$

where the second equality follows from Eq.(2.1); the first inequality uses a similar proof of [2, Theorem 12] and [44, Lemma 4]; the second inequality follows from Proposition 3.2 and $0 \leq \bar{C}_S^{l+1} \leq S$ is dependent on data \mathcal{S} ; and the third inequality follows from Lemma 4.2, [44, Lemma 4] together with the symmetric of the class $\{V_{1,\cdot}^l, x^l(d_{(s)}; \Theta_L^{\text{total}}) : x^l(\cdot; \Theta_L^{\text{total}}) \in \mathcal{F}^l, \|V_{1,\cdot}^l\|_1 \leq B_\Theta\}$.

Let $C_S^{l+1} = \min\{\sqrt{S} \frac{1+2\text{Lip}_\psi B_\Theta}{2(\text{Lip}_{\phi_1} \alpha + \text{Lip}_{\phi_2} \beta)}, \bar{C}_S^{l+1}\}$, $0 \leq l \leq L-1$. This truncation is introduced to ensure that the coefficients in the recursive inequality remain nonnegative, which is required for the application of the discrete Grönwall inequality. Then we get

$$\mathcal{R}_S(\mathcal{F}_1^{l+1}) \leq \mathcal{R}_S(\mathcal{F}_1^l) + \tau_L 2\text{Lip}_\psi B_\Theta^2 \mathcal{R}_S(\mathcal{F}_1^l) + \tau_L \frac{B_\Theta}{\sqrt{S}} \left(1 + 2\text{Lip}_\psi B_\Theta \right) - \tau_L B_\Theta \frac{(\text{Lip}_{\phi_1} \alpha + \text{Lip}_{\phi_2} \beta) C_S^{l+1}}{S},$$

where $0 \leq l \leq L-1$ and $0 \leq C_S^{l+1} \leq \min\{\sqrt{S} \frac{1+2\text{Lip}_\psi B_\Theta}{2(\text{Lip}_{\phi_1} \alpha + \text{Lip}_{\phi_2} \beta)}, S\}$. By applying Grönwall's inequality [13] to the inequality above together with $\tau_L \cdot L = T$, we get

$$\begin{aligned}
\mathcal{R}_S(\mathcal{F}_1^L) &\leq \left(\mathcal{R}_S(\mathcal{F}_1^0) + \frac{\tau_L L \cdot B_\Theta}{\sqrt{S}} (1 + 2\text{Lip}_\psi B_\Theta) \right) \exp(\tau_L L \cdot 2\text{Lip}_\psi B_\Theta^2) \\
&\quad - \frac{B_\Theta}{\sqrt{S}} \exp(\tau_L L \cdot 2\text{Lip}_\psi B_\Theta^2) \tau_L \sum_{l=1}^L \left(\frac{(\text{Lip}_{\phi_1} \alpha + \text{Lip}_{\phi_2} \beta) C_S^l}{\sqrt{S}} \right) \\
&= \left(\mathcal{R}_S(\mathcal{F}_1^0) + \frac{T B_\Theta}{\sqrt{S}} (1 + 2\text{Lip}_\psi B_\Theta) \right) \exp(2T \text{Lip}_\psi B_\Theta^2) \\
&\quad - \frac{B_\Theta}{\sqrt{S}} \exp(2T \text{Lip}_\psi B_\Theta^2) \tau_L \sum_{l=1}^L \left(\frac{(\text{Lip}_{\phi_1} \alpha + \text{Lip}_{\phi_2} \beta) C_S^l}{\sqrt{S}} \right).
\end{aligned}$$

Due to the lemma in [42, Lemma 26.11] and Eq.(3.2), we see

$$\mathcal{R}_S(\mathcal{F}_1^0) = \mathbb{E}_\epsilon \sup_{\max\{\|U_{1,\cdot}\|_1, |a_1|\} \leq B_\Theta} \frac{1}{S} \sum_{s=1}^S \epsilon_{(s)} \cdot \psi \circ (\mathbf{U}_{1,\cdot} d_{(s)} + a_1) \leq \text{Lip}_\psi B_\Theta \frac{B_{\text{in}} \sqrt{2 \log(2n_d)} + 1}{\sqrt{S}}.$$

It then follows from the above two inequalities that

$$(4.6) \quad \begin{aligned} \mathcal{R}_S(\mathcal{F}_1^L) &\leq \frac{B_\Theta}{\sqrt{S}} \left(\text{Lip}_\psi B_{\text{in}} \sqrt{2 \log(2n_d)} + 1 + T \cdot (1 + 2 \text{Lip}_\psi B_\Theta) \right) \exp(2T \text{Lip}_\psi B_\Theta^2) \\ &\quad - \frac{B_\Theta}{\sqrt{S}} \exp(2T \text{Lip}_\psi B_\Theta^2) \tau_L \sum_{l=1}^L \frac{(\text{Lip}_{\phi_1} \alpha + \text{Lip}_{\phi_2} \beta) C_S^l}{\sqrt{S}}. \end{aligned}$$

Hence, combining Eq.(4.4), Eq.(4.5), and Eq.(4.6), we complete the proof. \square

4.3. Proof of Theorem 3.9. In this subsection, we prove Theorem 3.9. Our approach is to transform the generalization problem of continuous dynamical systems into estimating the Rademacher complexity of discrete systems and to apply a convergence property from the discrete-time ResNet to the continuous-time ResNet. As in [24], we use the following definition to connect the discrete- and continuous-time learnable parameters.

DEFINITION 4.3. Let \mathcal{X} be a vector space. Partition the interval $[0, T]$ into L subintervals $\{[t_L^{l-1}, t_L^l]\}_{l=1}^{L-1} \cup [t_L^{L-1}, t_L^L]$, where $t_L^l := l \cdot T/L$. We define a sampling operator $\mathcal{T}_L : \mathcal{C}([0, T]; \mathcal{X}) \rightarrow \mathcal{X}^L$ for $\Xi \in \mathcal{C}([0, T]; \mathcal{X})$ by

$$\mathcal{T}_L(\Xi) = (\Xi(t_L^0), \dots, \Xi(t_L^{L-1})),$$

and define a piecewise constant extension operator $\bar{\mathcal{I}}_L : \mathcal{X}^L \rightarrow \mathcal{M}_L([0, T]; \mathcal{X})$ for any $\Xi_L = (\xi_L^0, \xi_L^1, \dots, \xi_L^{L-1}) \in \mathcal{X}^L$ by

$$(\bar{\mathcal{I}}_L \Xi_L)(t) = \sum_{l=0}^{L-2} \xi_L^l \mathbf{1}_{[t_L^l, t_L^{l+1})}(t) + \xi_L^{L-1} \mathbf{1}_{[t_L^{L-1}, t_L^L]}(t),$$

where $\mathcal{M}_L([0, T]; \mathcal{X})$ denotes the space of piecewise constant functions on $[0, T]$ with L pieces.

Using the above definition, we derive a convergence property between the state variables of discrete- and continuous-time ResNets.

LEMMA 4.4. Let assumptions $(A_1) - (A_3)$ hold and denote $t_L^l = l \tau_L = l \cdot \frac{T}{L}$, $0 \leq l \leq L$. Given a learnable parameter $\Theta^{\text{total}} = (\Theta^{\text{pre}}, \Theta) \in \Omega_{\Theta^{\text{total}}}$ and input $d \in \mathbb{R}^{n_d}$ such that $\|d\|_\infty \leq B_{\text{in}}$. Then there exists a parameter $\Theta_L^{\text{total}} = (\Theta^{\text{pre}}, \Theta_L) \in \Omega_{\Theta_L^{\text{total}}}$ and a constant C_1 such that

$$\|\bar{\mathcal{I}}_L \Theta_L - \Theta\|_{\mathcal{L}^2([0, T]; \mathcal{E})} \leq C_1 \tau_L^{1/2} \rightarrow 0 \text{ as } L \rightarrow \infty.$$

Moreover, for this Θ_L^{total} , there exists a constant $C_2 > 0$ such that

$$(4.7) \quad \sup_{1 \leq l \leq L} \sup_{t \in [t_L^{l-1}, t_L^l]} \|x^l(d; \Theta_L^{\text{total}}) - \mathbf{x}(t; \Theta^{\text{total}})\|_\infty \leq C_2 \tau_L^{1/2} \rightarrow 0 \text{ as } L \rightarrow \infty.$$

Proof. The proof primarily follows the approach in [46, 24]. For every $\Theta^{\text{total}} = (\Theta^{\text{pre}}, \Theta) \in \Omega_{\Theta^{\text{total}}}$, let $\Theta_L^{\text{total}} = (\Theta^{\text{pre}}, \Theta_L)$, where $\Theta_L = (\Theta_L^0, \Theta_L^1, \dots, \Theta_L^{L-1}) := \mathcal{T}_L(\Theta)$. By the definition of

$\Omega_{\Theta^{\text{total}}}$ and a similar proof of Morrey's inequality [29, Remark 11.35], we have for every $t, \hat{t} \in [0, T]$, $\|\Theta(t) - \Theta(\hat{t})\|_\infty \leq \bar{C}_1 |t - \hat{t}|^{1/2} \|D(\Theta)\|_{\mathcal{L}^2([0, T]; \mathcal{E})} \leq \bar{C}_1 B_\Theta |t - \hat{t}|^{1/2}$. Then

$$(4.8) \quad \begin{aligned} \|\bar{\mathcal{I}}_L \Theta_L - \Theta\|_{\mathcal{L}^2([0, T]; \mathcal{E})}^2 &= \sum_{l=0}^{L-1} \int_{t_L^l}^{t_L^{l+1}} \|\Theta(t_L^l) - \Theta(t)\|_\infty^2 dt \\ &\leq \sum_{l=0}^{L-1} \int_{t_L^l}^{t_L^{l+1}} \bar{C}_1^2 B_\Theta^2 |t_L^l - t| dt \leq C_1^2 \tau_L \rightarrow 0, \quad L \rightarrow \infty, \end{aligned}$$

where $C_1 = \sqrt{\frac{1}{2} \bar{C}_1^2 B_\Theta^2 T}$.

We next prove (4.7) for a such Θ_L^{total} . Let $e_L^l = \|\mathbf{x}^l(\mathbf{d}; \Theta_L^{\text{total}}) - \mathbf{x}(t_L^l; \mathbf{d}; \Theta^{\text{total}})\|_\infty$. Since the ResNets defined in Eq.(2.1) and Eq.(2.5) are special cases of the ResNet architectures considered in [24, Eq.(5) and Eq.(7)], it follows from the proof of [46, 24] that

$$(4.9) \quad \sup_{0 \leq l \leq L} e_L^l \leq \frac{\gamma_L M_2}{2} T \left(1 + \frac{M_1 T}{L}\right)^{2L} + \frac{M_2}{2\gamma_L} \|\Theta - \bar{\mathcal{I}}_L \Theta_L\|_{\mathcal{L}^2([0, T]; \mathcal{E})}^2 + M_3 \frac{T^2}{L} \left(1 + \frac{M_1 T}{L}\right)^L,$$

where M_1, M_2, M_3 are constants depending on $B_\Theta, B_{\text{in}}, T, \text{Lip}_\psi, \gamma_L > 0$ can be any constant. Taking $\gamma_L = \|\bar{\mathcal{I}}_L \Theta_L - \Theta\|_{\mathcal{L}^2([0, T]; \mathcal{E})}$ and by Eq.(4.8), we get

$$\sup_{0 \leq l \leq L} \|\mathbf{x}^l(\mathbf{d}; \Theta_L^{\text{total}}) - \mathbf{x}(t_L^l; \mathbf{d}; \Theta^{\text{total}})\|_\infty \leq M_4 \tau_L^{1/2},$$

where M_4 is a constant dependent on $B_\Theta, B_{\text{in}}, T, \text{Lip}_\psi$.

On the other hand,

$$(4.10) \quad \begin{aligned} \sup_{t \in [0, T]} \left\| \frac{d\mathbf{x}(t; \mathbf{d}; \Theta^{\text{total}})}{dt} \right\|_\infty &= \sup_{t \in [0, T]} \|\mathbf{W}(t)\psi \circ (\mathbf{V}(t)\mathbf{x}(t; \mathbf{d}; \Theta^{\text{total}}) + \mathbf{b}(t)) + \mathbf{c}(t)\|_\infty \\ &\leq \text{Lip}_\psi B_\Theta^2 (B_{\text{out}} + 1) + B_\Theta =: \text{Lip}_\mathbf{x}, \end{aligned}$$

where B_{out} is a constant given in Lemma 4.1. Therefore, combining Eq.(4.9) and Eq.(4.10) gives

$$(4.11) \quad \begin{aligned} &\sup_{t \in [t_L^{l-1}, t_L^l]} \|\mathbf{x}(t; \mathbf{d}; \Theta^{\text{total}}) - \mathbf{x}^l(\mathbf{d}; \Theta_L^{\text{total}})\|_\infty \\ &\leq \sup_{t \in [t_L^{l-1}, t_L^l]} (\|\mathbf{x}(t; \mathbf{d}; \Theta^{\text{total}}) - \mathbf{x}(t_L^l; \mathbf{d}; \Theta^{\text{total}})\|_\infty + \|\mathbf{x}(t_L^l; \mathbf{d}; \Theta^{\text{total}}) - \mathbf{x}^l(\mathbf{d}; \Theta_L^{\text{total}})\|_\infty) \\ &\leq \text{Lip}_\mathbf{x} \tau_L + M_4 \tau_L^{1/2}. \end{aligned}$$

Letting $C_2 = \text{Lip}_\mathbf{x} \sqrt{T} + M_4$ completes the proof. \square

We now prove Theorem 3.9.

Proof. (Proof of Theorem 3.9) We divide the proof into two steps.

Step 1. We show the boundedness of the loss function and apply the theorem in [42, Theorem 26.5] to get a Rademacher complexity upper bound of the generalization gap. Similar to the discussion in the proof of Theorem 3.5, the loss function ℓ is bounded by a constant B_ℓ dependent on $T, B_{\text{in}}, B_\Theta, \text{Lip}_\psi$. Therefore, for any $0 < \delta < 1$, with probability $1 - \delta$ that

$$(4.12) \quad GE_S(\mathbf{x}(T; \cdot; \Theta^{\text{total}})) \leq 2\mathcal{R}_S(\ell \circ \mathcal{F}^T) + 4B_\ell \sqrt{\frac{2 \log(4/\delta)}{S}}, \quad \forall \mathbf{x}(T; \cdot; \Theta^{\text{total}}) \in \mathcal{F}^T,$$

due to [42, Theorem 26.5]. Here $\ell \circ \mathcal{F}^T = \{f(\cdot, \cdot) = \ell(\mathbf{x}(T; \cdot; \boldsymbol{\Theta}^{\text{total}}), \cdot) : \mathbf{x}(T; \cdot; \boldsymbol{\Theta}^{\text{total}}) \in \mathcal{F}^T\}$.

Step 2. We estimate the Rademacher complexity $\mathcal{R}_S(\ell \circ \mathcal{F}^T)$. Similar to the discussion in Step 2 of the proof of Theorem 3.5, we have

$$\begin{aligned}
\mathcal{R}_S(\ell \circ \mathcal{F}^T) &= \frac{1}{S} \mathbb{E}_\epsilon \sup_{\ell \circ \mathbf{x}(T; \cdot; \boldsymbol{\Theta}^{\text{total}}) \in \ell \circ \mathcal{F}^T} \sum_{s=1}^S \varepsilon_{(s)} \cdot \ell(\mathbf{x}(T; \mathbf{d}_{(s)}; \boldsymbol{\Theta}^{\text{total}}), \mathbf{g}_{(s)}) \\
&= \frac{1}{S} \mathbb{E}_\epsilon \sup_{\mathbf{x}(T; \cdot; \boldsymbol{\Theta}^{\text{total}}) \in \mathcal{F}^T} \sum_{s=1}^S \varepsilon_{(s)} \cdot \ell(\mathbf{x}(T; \mathbf{d}_{(s)}; \boldsymbol{\Theta}^{\text{total}}), \mathbf{g}_{(s)}) \\
(4.13) \quad &\leq \sqrt{2} B_\kappa \frac{1}{S} \mathbb{E}_\epsilon \sup_{\mathbf{x}_k(T; \cdot; \boldsymbol{\Theta}^{\text{total}}) \in \mathcal{F}_k^T} \sum_{s=1}^S \sum_{k=1}^n \epsilon_{(sk)} \cdot \mathbf{x}_k(T; \mathbf{d}_{(s)}; \boldsymbol{\Theta}^{\text{total}}) \\
&\leq \sqrt{2} B_\kappa \sum_{k=1}^n \mathbb{E}_{\epsilon_{k,\cdot}} \sup_{\mathbf{x}_k(T; \cdot; \boldsymbol{\Theta}^{\text{total}}) \in \mathcal{F}_k^T} \frac{1}{S} \sum_{s=1}^S \epsilon_{(sk)} \cdot \mathbf{x}_k(T; \mathbf{d}_{(s)}; \boldsymbol{\Theta}^{\text{total}}) \\
&= \sqrt{2} B_\kappa \sum_{k=1}^n \mathcal{R}_S(\mathcal{F}_k^T),
\end{aligned}$$

with $\epsilon_{k,\cdot} = \{\epsilon_{1k}, \dots, \epsilon_{Sk}\}$, where the first inequality is due to [35, Corollary 1].

To apply the result in Theorem 3.5, we let $t_L^l = l\tau_L = l \cdot \frac{T}{L}$, $0 \leq l \leq L$. Then there are constants c_1, c_2 independent of L such that

$$\|\bar{\mathcal{I}}_L \mathcal{T}_L(\boldsymbol{\Theta}) - \boldsymbol{\Theta}\|_{\mathcal{L}^2([0, T]; \mathcal{E})}^2 \leq c_1 \tau_L, \forall \boldsymbol{\Theta} \in \Omega_{\boldsymbol{\Theta}}$$

and also

$$(4.14) \quad \|\mathbf{x}(T; \mathbf{d}; \boldsymbol{\Theta}^{\text{total}}) - \mathbf{x}^L(\mathbf{d}; (\boldsymbol{\Theta}^{\text{pre}}, \mathcal{T}_L(\boldsymbol{\Theta})))\|_\infty \leq c_2 \tau_L^{\frac{1}{2}}, \forall \mathbf{d} \in \mathbb{R}^{n_d}, \forall \boldsymbol{\Theta} \in \Omega_{\boldsymbol{\Theta}}$$

by using Lemma 4.4. Hence, noting $(\boldsymbol{\Theta}^{\text{pre}}, \mathcal{T}_L(\boldsymbol{\Theta})) \in \Omega_{\boldsymbol{\Theta}^{\text{total}}}$ for all $(\boldsymbol{\Theta}^{\text{pre}}, \boldsymbol{\Theta}) \in \Omega_{\boldsymbol{\Theta}}$ and applying Eq.(4.6) and Eq.(4.14), we get

$$\begin{aligned}
\mathcal{R}_S(\mathcal{F}_k^T) &= \frac{1}{S} \mathbb{E}_\epsilon \sup_{\mathbf{x}_k(T; \cdot; \boldsymbol{\Theta}^{\text{total}}) \in \mathcal{F}_k^T} \sum_{s=1}^S \varepsilon_{(s)} \mathbf{x}_k(T; \mathbf{d}_{(s)}; \boldsymbol{\Theta}^{\text{total}}) \\
&\leq \frac{1}{S} \mathbb{E}_\epsilon \left[\sup_{\boldsymbol{\Theta}^{\text{total}} \in \Omega_{\boldsymbol{\Theta}^{\text{total}}}} \sum_{s=1}^S \varepsilon_{(s)} \left(\mathbf{x}_k(T; \mathbf{d}_{(s)}; \boldsymbol{\Theta}^{\text{total}}) - \mathbf{x}_k^L(\mathbf{d}_{(s)}; (\boldsymbol{\Theta}^{\text{pre}}, \mathcal{T}_L(\boldsymbol{\Theta}))) \right) \right] \\
&\quad + \frac{1}{S} \mathbb{E}_\epsilon \sup_{\boldsymbol{\Theta}^{\text{total}} \in \Omega_{\boldsymbol{\Theta}^{\text{total}}}} \sum_{s=1}^S \varepsilon_{(s)} \mathbf{x}_k^L(\mathbf{d}_{(s)}; (\boldsymbol{\Theta}^{\text{pre}}, \mathcal{T}_L(\boldsymbol{\Theta}))) \\
&\leq c_2 \sqrt{\tau_L} + \frac{1}{S} \mathbb{E}_\epsilon \sup_{\mathbf{x}_k^L(\cdot; \boldsymbol{\Theta}_L^{\text{total}}) \in \mathcal{F}_k^L} \sum_{s=1}^S \varepsilon_{(s)} \mathbf{x}_k^L(\mathbf{d}_{(s)}; \boldsymbol{\Theta}_L^{\text{total}}) \\
&= c_2 \sqrt{\tau_L} + \mathcal{R}_S(\mathcal{F}_k^L) \\
&\leq c_2 \sqrt{\tau_L} + \frac{B_{\boldsymbol{\Theta}}}{\sqrt{S}} \left(\text{Lip}_\psi B_{\text{in}} \sqrt{2 \log(2n_d)} + 1 + T(1 + 2\text{Lip}_\psi B_{\boldsymbol{\Theta}}) \right) \exp(2T \text{Lip}_\psi B_{\boldsymbol{\Theta}}^2)
\end{aligned}$$

$$- \frac{B_{\Theta}}{\sqrt{S}} \exp(2T \text{Lip}_{\psi} B_{\Theta}^2) \tau_L \sum_{l=1}^L \frac{(\text{Lip}_{\phi_1} \alpha + \text{Lip}_{\phi_2} \beta) C_{\mathcal{S}}^l}{\sqrt{S}},$$

where $1 \leq k \leq n$, $0 \leq C_{\mathcal{S}}^l \leq \min\{\sqrt{S} \frac{1+2\text{Lip}_{\psi} B_{\Theta}}{2(\text{Lip}_{\phi_1} \alpha + \text{Lip}_{\phi_2} \beta)}, S\}$.

Since $\tau_L = \frac{T}{L}$, letting $L \rightarrow \infty$, possibly along a subsequence, we conclude that there exists a constant $C_{\mathcal{S}}$ dependent on data \mathcal{S} such that

$$\begin{aligned} \mathcal{R}_{\mathcal{S}}(\mathcal{F}_k^T) &\leq \frac{B_{\Theta}}{\sqrt{S}} \left(\text{Lip}_{\psi} B_{\text{in}} \sqrt{2 \log(2n_d)} + 1 + T(1 + \text{Lip}_{\psi} B_{\Theta}) \right) \exp(T \text{Lip}_{\psi} B_{\Theta}^2) \\ &\quad - \frac{B_{\Theta} (\text{Lip}_{\phi_1} \alpha + \text{Lip}_{\phi_2} \beta) \exp(T \text{Lip}_{\psi} B_{\Theta}^2) T}{S} C_{\mathcal{S}}, \end{aligned}$$

where $1 \leq k \leq n$, $0 \leq C_{\mathcal{S}} \leq \min\{\sqrt{S} \frac{1+\text{Lip}_{\psi} B_{\Theta}}{\text{Lip}_{\phi_1} \alpha + \text{Lip}_{\phi_2} \beta}, S\}$. Substituting the above inequality into Eq.(4.13) and combining Eq.(4.12) completes the proof. \square

5. Experiments. In this section, we conduct experiments to evaluate the generalization ability of ResNets within the dynamical system modeling framework. Specifically, we examine how generalization is affected by varying the number of training samples and the number of neural network layers. We also investigate the influence of activation functions on the generalization behavior of ResNets from the perspective of the proposed theoretical framework. All ResNets are trained for 30 epochs on the MNIST dataset and 120 epochs on the CIFAR10 and CIFAR100 datasets using the SGD optimizer with an initial learning rate of 0.01 and a momentum of 0.9. All training and testing procedures are implemented using PyTorch on NVIDIA GeForce RTX 3090 GPUs. Our code is available at “<https://github.com/Huangjsh15/Dynamical-ResNet.git>”.

5.1. A test on the influence of training sample size S . Assume that $S_{\mathfrak{D}}$ is a large number such that $S_{\mathfrak{D}} \gg S$. Let the training and testing samples used in experiments be $\mathcal{S} = \{(d_{(s)}, g_{(s)})\}_{s=1}^{S_{\mathfrak{D}}}$ and $\bar{\mathcal{S}} = \{(d_{(s)}, g_{(s)})\}_{s=S+1}^{S+S}$, respectively. Following the definition of the generalization gap in (2.11), we derive

$$\begin{aligned} GE_{\mathcal{S}}(x^L(\cdot; \Theta_L^{\text{total}})) &= \mathfrak{R}_{\mathfrak{D}}(x^L(\cdot; \Theta_L^{\text{total}})) - \hat{\mathfrak{R}}_{\mathcal{S}}(x^L(\cdot; \Theta_L^{\text{total}})) \\ &\approx \frac{1}{S_{\mathfrak{D}}} \sum_{s=1}^{S_{\mathfrak{D}}} \ell(x^L(d_{(s)}; \Theta^{\text{total}}), g_{(s)}) - \frac{1}{S} \sum_{s=1}^S \ell(x^L(d_{(s)}; \Theta^{\text{total}}), g_{(s)}) \\ &= -\frac{S_{\mathfrak{D}} - S}{S_{\mathfrak{D}}} \frac{1}{S} \sum_{s=1}^S \ell(x^L(d_{(s)}; \Theta^{\text{total}}), g_{(s)}) + \frac{S_{\mathfrak{D}} - S}{S_{\mathfrak{D}}} \frac{1}{S_{\mathfrak{D}} - S} \sum_{s=S+1}^{S_{\mathfrak{D}}} \ell(x^L(d_{(s)}; \Theta^{\text{total}}), g_{(s)}) \\ &\approx \frac{S_{\mathfrak{D}} - S}{S_{\mathfrak{D}}} (\hat{\mathfrak{R}}_{\text{test}} - \hat{\mathfrak{R}}_{\text{train}}) \approx \hat{\mathfrak{R}}_{\text{test}} - \hat{\mathfrak{R}}_{\text{train}}, \end{aligned}$$

where the training loss $\hat{\mathfrak{R}}_{\text{train}} = \hat{\mathfrak{R}}_{\mathcal{S}}(x^L(\cdot; \Theta_L^{\text{total}})) = \frac{1}{S} \sum_{s=1}^S \ell(x^L(d_{(s)}; \Theta^{\text{total}}), g_{(s)})$ and testing loss $\hat{\mathfrak{R}}_{\text{test}} = \frac{1}{S} \sum_{s=S+1}^{S+S} \ell(x^L(d_{(s)}; \Theta^{\text{total}}), g_{(s)}) \approx \frac{1}{S_{\mathfrak{D}} - S} \sum_{s=S+1}^{S_{\mathfrak{D}}} \ell(x^L(d_{(s)}; \Theta^{\text{total}}), g_{(s)})$ since we assume the samples are i.i.d. distributed. This derivation shows that the difference between the testing and training losses can approximate the generalization gap (2.11). Therefore, the result in Theorem 3.5 can be empirically validated by measuring the quantity $\hat{\mathfrak{R}}_{\text{test}} - \hat{\mathfrak{R}}_{\text{train}}$ under varying training sample size S .

In Figure 1, we present the average testing-training loss gap of ResNets $\hat{\mathfrak{R}}_{\text{test}} - \hat{\mathfrak{R}}_{\text{train}}$ at the last 10 epochs for ResNets trained on the MNIST, CIFAR10, and CIFAR100 datasets. Guided by Theorem 3.5, which suggests an $O(\frac{1}{\sqrt{S}})$ generalization rate, we fit the empirical gap using the least squares method with function $h_{\mu}(S) = \mu/\sqrt{S}$. The fitted curves exhibit close agreement with the theoretical prediction, thereby validating the asymptotic rate suggested by our bound. Final test accuracies for both datasets are summarized in Table 3. The results further confirm that the generalization error decreases as the number of training samples increases.

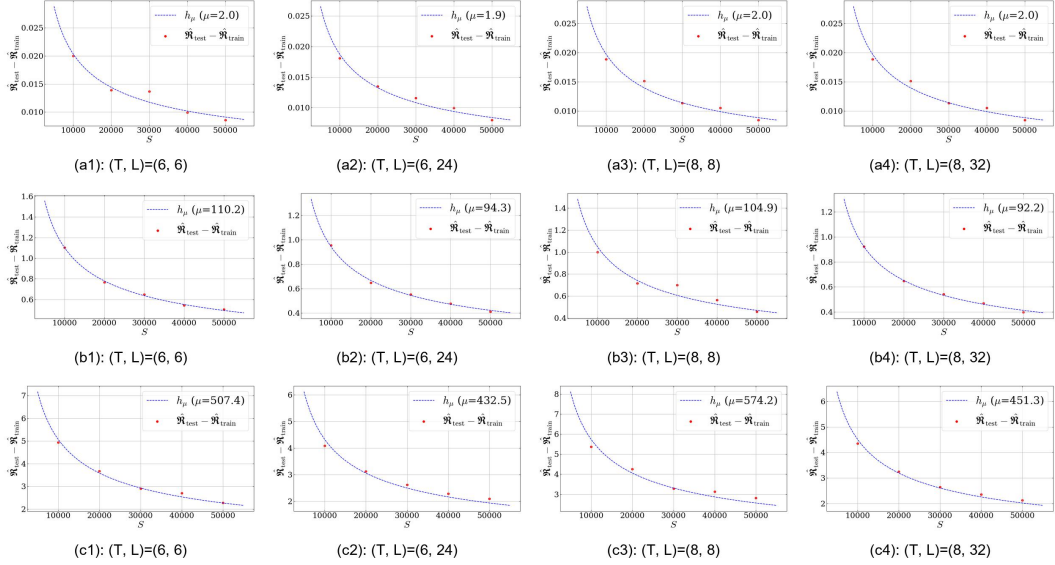


FIG. 1. Average testing-training loss gap of ResNets with $(T, L) = (6, 6)$, $(6, 24)$ and $(T, L) = (8, 8)$, $(8, 32)$ at last 10 epochs versus training sample size S , along with least-squares fitting using $h_{\mu}(S) = \mu/\sqrt{S}$. Plots (a1)-(a4) show results of ResNets on MNIST. Plots (b1)-(b4) show results of ResNets on CIFAR10. Plots (c1)-(c4) show results of ResNets on CIFAR100. The generalization gap decreases with increasing S , closely matching the theoretical rate of $O(1/\sqrt{S})$.

5.2. A test on the layer number of ResNets. Theorem 3.5 and Theorem 3.9 reveal how the generalization bounds behave as the depth of ResNets increases. To empirically validate these theoretical results, we conduct experiments by progressively increasing the layer number L of the ResNets. The training loss and testing classification accuracy over epochs are plotted in Figure 2 and Figure 3, respectively. The results show that as L increases, both training loss and testing accuracy of the discrete-time ResNet tend to converge. This empirical behavior is consistent with the theoretical predictions, supporting the connection between network depth, convergence, and generalization performance.

5.3. Influence of activation functions with structured decomposition. In this subsection, we further investigate the influence of activation functions on the generalization behavior of ResNets within the proposed theoretical framework. In particular, we focus on activation functions that admit a structured decomposition of the form in Definition 3.1.

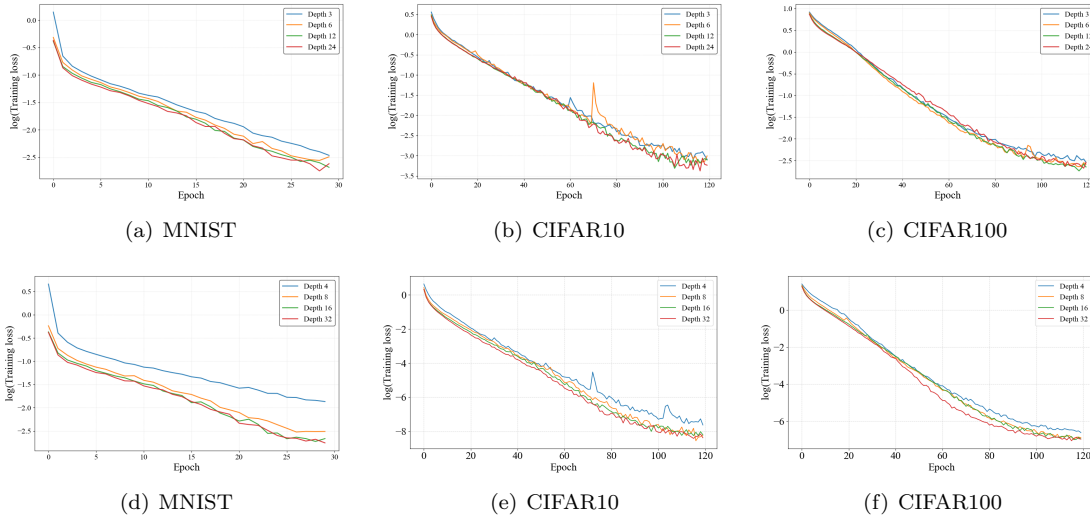


FIG. 2. Training loss of ResNets with varying layer numbers in the deep-layer limit regime. The first row corresponds to $T = 6$ with $L = 3, 6, 12, 24$, and the second row corresponds to $T = 8$ with $L = 4, 8, 16, 32$. Across all datasets (MNIST, CIFAR10, CIFAR100), the training loss exhibits convergence behavior as the number of layers increases, supporting the depth-stability predicted by our theoretical analysis.

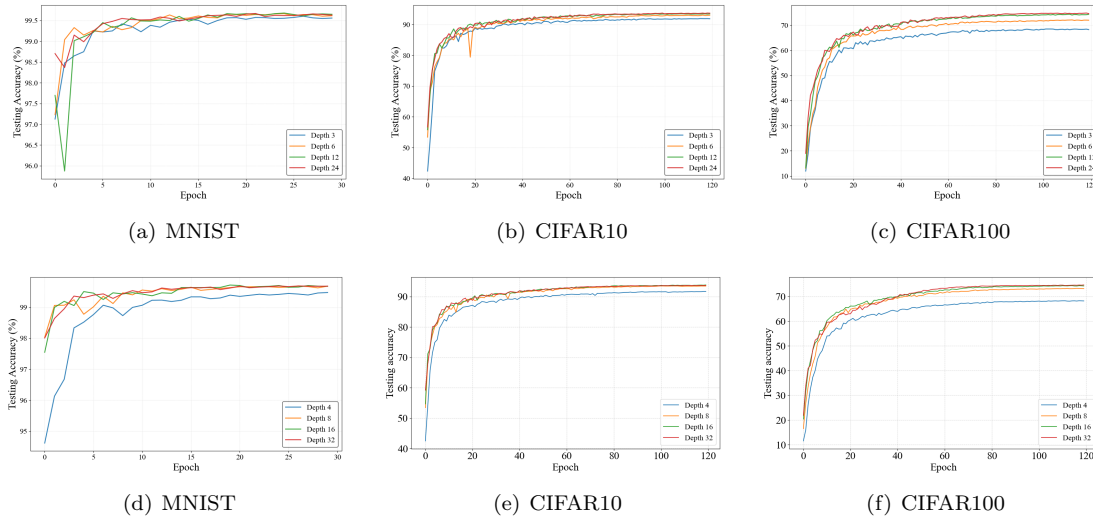


FIG. 3. Top-1 image classification accuracy of ResNets with varying layer numbers in the deep-layer limit regime. The first row corresponds to $T = 6$ with $L = 3, 6, 12, 24$, and the second row corresponds to $T = 8$ with $L = 4, 8, 16, 32$. Across all datasets (MNIST, CIFAR10, CIFAR100), the testing accuracy exhibits convergence behavior as the number of layers increases, supporting the depth-stability predicted by our theoretical analysis.

TABLE 3

The top-1 image classification testing accuracy by trained ResNets with $(T, L) = (6, 6), (6, 24)$ and $(T, L) = (8, 8), (8, 32)$ on MNIST, CIFAR10 and CIFAR100 datasets with different training sample sizes S .

		Testing accuracy				
(T, L)	Samples	10^4	$2 \cdot 10^4$	$3 \cdot 10^4$	$4 \cdot 10^4$	$5 \cdot 10^4$
(6, 6)	MNIST	99.549	99.589	99.639	99.669	99.629
	CIFAR10	84.375	89.083	90.865	92.348	92.839
	CIFAR100	49.189	59.165	66.216	68.139	72.516
(6, 24)	MNIST	99.479	99.589	99.579	99.659	99.669
	CIFAR10	84.896	89.694	91.526	92.728	93.58
	CIFAR100	53.405	64.323	69.591	72.596	74.72
(8, 8)	MNIST	99.489	99.589	99.619	99.579	99.669
	CIFAR10	84.143	89.329	90.995	92.474	93.5
	CIFAR100	49.211	61.793	66.743	69.455	73.177
(8, 32)	MNIST	99.409	99.589	99.639	99.589	99.669
	CIFAR10	85.116	89.463	91.797	92.768	93.82
	CIFAR100	53.486	64.193	69.321	71.855	74.509

We consider a class of activation functions that explicitly admit such a decomposition:

$$(5.1) \quad \psi_{a,b;\alpha,\beta}(x) = \begin{cases} a(x - \alpha), & x \geq \alpha, \\ 0, & -\beta < x < \alpha, \\ b(x + \beta), & x \leq -\beta, \end{cases}$$

where $\alpha, \beta > 0$. This formulation introduces an explicit dead-zone region (β, α) and allows us to control the slope parameters on both sides. Specifically, we consider two representative cases of (5.1). The first one is $\psi_{1,0.05;0,0}(\cdot)$, which reduces to the standard leaky ReLU activation with slope parameter 0.05, i.e.,

$$\psi(x) = \begin{cases} x, & x \geq 0, \\ 0.05 \cdot x, & x < 0. \end{cases}$$

The second case is $\psi_{1,0.05;\alpha,\beta}(\cdot)$, where α and β are treated as learnable parameters. By varying α and β , the activation introduces a controllable dead-zone region.

To remain consistent with the theoretical setting, the activation parameters α and β are shared across all layers, i.e., the same activation function is used throughout the network. For each network configuration, we evaluate the empirical generalization gap $\hat{\mathfrak{R}}_{\text{test}} - \hat{\mathfrak{R}}_{\text{train}}$. Figure 4 reports these testing–training loss gaps for different activation functions on three datasets. We observe that, in the later stage of training, ResNets equipped with the activation function $\psi_{1,0.05;\alpha,\beta}(\cdot)$ tend to yield smaller generalization gaps compared to the standard leaky ReLU on CIFAR10 and CIFAR100. This indicates improved generalization performance and provides empirical evidence for the effect of the non-positive term appearing in Theorem 3.5. In particular, the presence of a structured decomposition and an explicit dead-zone leads to a sharper estimate than bounds that rely solely on the global Lipschitz constant of the activation function. Overall, these results indicate that the proposed generalization theory not only captures the dependence on network depth and sample size,

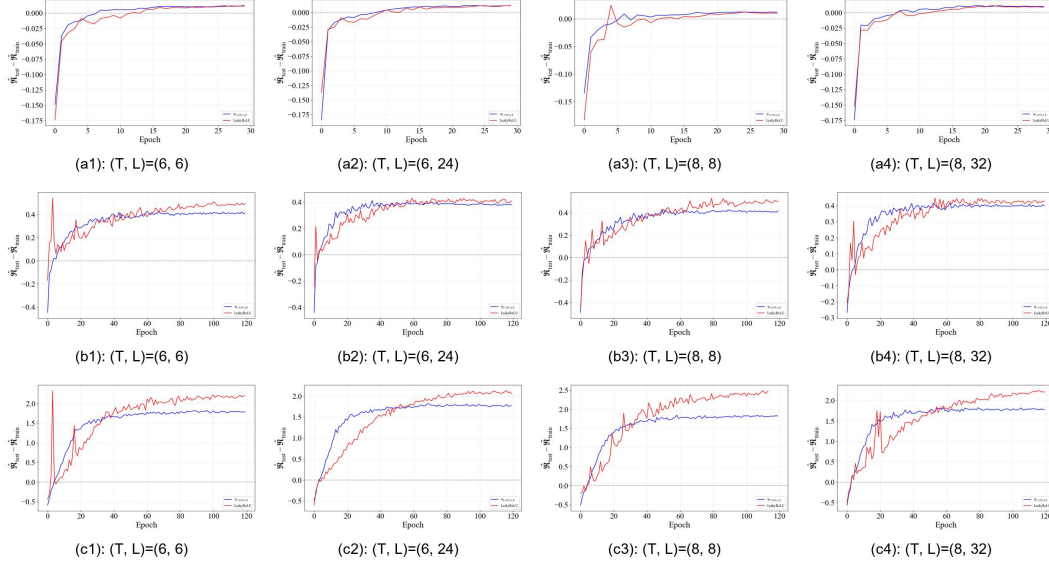


FIG. 4. Empirical generalization gap $\hat{\mathfrak{R}}_{\text{test}} - \hat{\mathfrak{R}}_{\text{train}}$ versus training epoch for ResNets with different (T, L) configurations. The first row corresponds to MNIST, the second row to CIFAR10, and the third row to CIFAR100. ResNets equipped with activation functions admitting a structured decomposition exhibit smaller generalization gaps on CIFAR10 and CIFAR100 in the later stage of training.

but also provides a meaningful characterization of how structured activation functions influence the generalization behavior of ResNets.

6. Conclusion. In this work, we investigated the generalization properties of deep residual networks through the lens of dynamical systems. By leveraging a new contraction-type inequality for activation functions, Rademacher complexity theory, and the convergence behavior of ResNets in the deep-layer limit, we derived new generalization bounds for both discrete- and continuous-time ResNets. These bounds attain a complexity order of $O(1/\sqrt{S})$ and remain uniformly bounded as depth increases, enabling an asymptotic characterization of generalization behavior with respect to network depth. Our discrete-time bound further incorporates a structure-dependent negative term, which can potentially tighten estimates under suitable conditions. Overall, this dynamical system framework offers a unified and theoretically grounded perspective on the interplay between architectural stability, depth, and generalization, and helps to close the order gap between the existing generalization analyses for discrete- and continuous-time ResNets.

Appendix A. Definition of Rademacher complexity.

DEFINITION A.1. The (empirical) Rademacher complexity of the function class \mathcal{F} for i.i.d. sample $\mathcal{Z} = \{z_{(1)}, z_{(2)}, \dots, z_{(S)}\}$ from \mathfrak{B} is

$$\mathcal{R}_{\mathcal{Z}}(\mathcal{F}) = \frac{1}{S} \mathbb{E}_{\boldsymbol{\varepsilon}} \left[\sup_{f \in \mathcal{F}} \sum_{s=1}^S \varepsilon_{(s)} f(z_{(s)}) \right],$$

where the expectation is taken over $\boldsymbol{\varepsilon} = \{\varepsilon_{(1)}, \varepsilon_{(2)}, \dots, \varepsilon_{(S)}\}$ and $\varepsilon_{(s)}$ ($1 \leq s \leq S$) are independently

and uniformly distributed over $\{-1, 1\}$.

For convenience, we denote $\boldsymbol{\varepsilon} = \{\varepsilon_{(1)}, \varepsilon_{(2)}, \dots, \varepsilon_{(S)}\}$ and $\boldsymbol{\epsilon} = \{\epsilon_{(11)}, \dots, \epsilon_{(S1)}; \dots; \epsilon_{(1N)}, \dots, \epsilon_{(SN)}\}$, where $\{\varepsilon_{(s)}\}_s$ and $\{\epsilon_{(sj)}\}_{s,j}$ are independently and uniformly distributed over $\{-1, 1\}$. Also, for the convenience of readers, several key referred results are provided in the supplementary material.

Acknowledgments. This work was partially supported by the National Natural Science Foundation of China (grant 12271273) and the Key Program (21JCZDJC00220) of the Natural Science Foundation of Tianjin, China.

REFERENCES

- [1] P. L. BARTLETT, D. J. FOSTER, AND M. J. TELGARSKY, Spectrally-normalized margin bounds for neural networks, *Advances in Neural Information Processing Systems*, 30 (2017).
- [2] P. L. BARTLETT AND S. MENDELSON, Rademacher and gaussian complexities: Risk bounds and structural results, *Journal of Machine Learning Research*, 3 (2002), pp. 463–482.
- [3] P. L. BARTLETT AND R. C. WILLIAMSON, The vc dimension and pseudodimension of two-layer neural networks with discrete inputs, *Neural Computation*, 8 (1996), pp. 625–628.
- [4] A. BECK, First-order methods in optimization, SIAM, 2017.
- [5] M. BENNING, E. CELLEDONI, M. J. EHRHARDT, B. OWREN, AND C.-B. SCHÖNLIEB, Deep learning as optimal control problems: Models and numerical methods, *Journal of Computational Dynamics*, 6 (2019), pp. 171–198.
- [6] L. BLEISTEIN AND A. GUILLOUX, On the generalization capacities of neural controlled differential equations, in *Workshop on New Frontiers in Learning, Control, and Dynamical Systems at the International Conference on Machine Learning (ICML 2023)*, 2023.
- [7] O. BOUSQUET AND A. ELISSEEFF, Stability and generalization, *Journal of Machine Learning Research*, 2 (2002), pp. 499–526.
- [8] R. T. CHEN, Y. RUBANOVA, J. BETTENCOURT, AND D. K. DUVENAUD, Neural ordinary differential equations, *Advances in Neural Information Processing Systems*, 31 (2018).
- [9] X. CHEN, Y. ZHANG, C. REISINGER, AND L. SONG, Understanding deep architecture with reasoning layer, in *Advances in Neural Information Processing Systems*, 2020.
- [10] D.-A. CLEVERT, Fast and accurate deep network learning by exponential linear units (elus), arXiv preprint arXiv:1511.07289, (2015).
- [11] W. E, A proposal on machine learning via dynamical systems, *Communications in Mathematics and Statistics*, 1 (2017), pp. 1–11.
- [12] W. E, C. MA, AND Q. WANG, Rademacher complexity and the generalization error of residual networks, *Communications in Mathematical Sciences*, 18 (2020), pp. 1755–1774.
- [13] E. EMMRICH, Discrete versions of Gronwall’s lemma and their application to the numerical analysis of parabolic problems, Techn. Univ., 1999.
- [14] X. GLOROT, A. BORDES, AND Y. BENGIO, Deep sparse rectifier neural networks, in *Proceedings of the Fourteenth International Conference on Artificial Intelligence and Statistics, JMLR Workshop and Conference Proceedings*, 2011, pp. 315–323.
- [15] P. GOLDBERG AND M. JERRUM, Bounding the vapnik-chervonenkis dimension of concept classes parameterized by real numbers, *Machine Learning*, 18 (1995), pp. 131–148.
- [16] I. GOODFELLOW, Y. BENGIO, AND A. COURVILLE, Deep learning, MIT press, 2016.
- [17] P. GROHS AND G. KUTYNIOK, Mathematical aspects of deep learning, Cambridge University Press, 2022.
- [18] S. GUNTHER, L. RUTHOTTO, J. B. SCHRODER, E. C. CYR, AND N. R. GAUGER, Layer-parallel training of deep residual neural networks, *SIAM Journal on Mathematics of Data Science*, 2 (2020), pp. 1–23.
- [19] E. HABER AND L. RUTHOTTO, Stable architectures for deep neural networks, *Inverse Problems*, 34 (2017), p. 014004.
- [20] J. HANSON AND M. RAGINSKY, Rademacher complexity of neural odes via chen-fliess series, in *6th Annual Learning for Dynamics & Control Conference*, PMLR, 2024, pp. 758–769.
- [21] F. HE, T. LIU, AND D. TAO, Why resnet works? residuals generalize, *IEEE Transactions on Neural Networks and Learning Systems*, 31 (2020), pp. 5349–5362.
- [22] K. HE, X. ZHANG, S. REN, AND J. SUN, Delving deep into rectifiers: Surpassing human-level performance on imagenet classification, in *Proceedings of the IEEE International Conference on Computer Vision*, 2015,

- pp. 1026–1034.
- [23] K. HE, X. ZHANG, S. REN, AND J. SUN, Deep residual learning for image recognition, in Proceedings of the IEEE Conference on Computer Vision and Pattern Recognition, 2016, pp. 770–778.
 - [24] J. HUANG, Y. GAO, AND C. WU, On dynamical system modeling of learned primal-dual with a linear operator \mathcal{K} : stability and convergence properties, Inverse Problems, 40 (2024), p. 075006.
 - [25] J. HUANG, H. SU, X.-C. TAI, AND C. WU, Mathematical modeling and convergence analysis of deep neural networks with dense layer connectivities, Submitted, (2024).
 - [26] E. KÖBLER, A. EFFLAND, K. KUNISCH, AND T. POCK, Total deep variation for linear inverse problems, in IEEE Conference on Computer Vision and Pattern Recognition, 2020, pp. 7549–7558.
 - [27] I. KUZBORSKIJ AND C. LAMPERT, Data-dependent stability of stochastic gradient descent, in International Conference on Machine Learning, PMLR, 2018, pp. 2815–2824.
 - [28] Y. LECUN, Y. BENGIO, AND G. HINTON, Deep learning, Nature, 521 (2015), pp. 436–444.
 - [29] G. LEONI, A first course in Sobolev spaces, American Mathematical Soc., 2017.
 - [30] Q. LI, T. LIN, AND Z. SHEN, Deep learning via dynamical systems: An approximation perspective, Journal of the European Mathematical Society, 25 (2022), pp. 1671–1709.
 - [31] X. LI, J. LU, Z. WANG, J. HAUPT, AND T. ZHAO, On tighter generalization bound for deep neural networks: Cnns, resnets, and beyond, arXiv preprint arXiv:1806.05159, (2018).
 - [32] Z. LI, J. HAN, E. WEINAN, AND Q. LI, Approximation and optimization theory for linear continuous-time recurrent neural networks, Journal of Machine Learning Research, 23 (2022), pp. 1–85.
 - [33] Y. LU, A. ZHONG, Q. LI, AND B. DONG, Beyond finite layer neural networks: Bridging deep architectures and numerical differential equations, in Proceedings of Machine Learning Research, vol. 80, PMLR, 2018, pp. 3282–3291.
 - [34] P. MARION, Generalization bounds for neural ordinary differential equations and deep residual networks, Advances in Neural Information Processing Systems, 36 (2023), pp. 48918–48938.
 - [35] A. MAURER, A vector-contraction inequality for rademacher complexities, in Algorithmic Learning Theory: 27th International Conference, Springer, 2016, pp. 3–17.
 - [36] B. NEYSHABUR, S. BHOJANAPALLI, AND N. SREBRO, A pac-bayesian approach to spectrally-normalized margin bounds for neural networks, in International Conference on Learning Representations, 2018.
 - [37] B. NEYSHABUR, R. TOMIOKA, AND N. SREBRO, Norm-based capacity control in neural networks, in Conference on Learning Theory, PMLR, 2015, pp. 1376–1401.
 - [38] V. PANDEY, Overcoming overfitting and large weight update problem in linear rectifiers: Thresholded exponential rectified linear units, arXiv preprint arXiv:2006.02797, (2020).
 - [39] P. PAPPAS AND C. MUIR, Predict globally, correct locally: Parallel-in-time optimization of neural networks, Automatica, 171 (2025), <https://doi.org/10.1016/j.automatica.2024.111976>.
 - [40] L. RUTHOTTO AND E. HABER, Deep neural networks motivated by partial differential equations, Journal of Mathematical Imaging and Vision, 62 (2020), pp. 352–364.
 - [41] E. SCHNOOR, A. BEHBOODI, AND H. RAUHUT, Generalization error bounds for iterative recovery algorithms unfolded as neural networks, Information and Inference: A Journal of the IMA, 12 (2023), pp. 2267–2299.
 - [42] S. SHALEV-SHWARTZ AND S. BEN-DAVID, Understanding machine learning: From theory to algorithms, Cambridge University Press, 2014.
 - [43] A. SHERSTINSKY, Fundamentals of recurrent neural network (rnn) and long short-term memory (lstm) network, Physica D: Nonlinear Phenomena, 404 (2020), p. 132306.
 - [44] A. SHULTZMAN, E. AZAR, M. R. RODRIGUES, AND Y. C. EL-DAR, Generalization and estimation error bounds for model-based neural networks, in International Conference on Learning Representations, 2023.
 - [45] J. SOKOLIC, R. GIRYES, G. SAPIRO, AND M. RODRIGUES, Generalization error of invariant classifiers, in Artificial Intelligence and Statistics, PMLR, 2017, pp. 1094–1103.
 - [46] M. THORPE AND Y. VAN GENNIP, Deep limits of residual neural networks, Research in the Mathematical Sciences, 10 (2023), p. 6.
 - [47] R. VERSHYNIN, High-dimensional probability: An introduction with applications in data science, vol. 47, Cambridge University Press, 2018.